Oceano Dunes Pilot Projects

Final Project Report

September 15, 2011

Nicholas Lancaster [(1)], John Gillies[(2)], Vic Etyemezian[(2)], George Nikolich[(2)]

[(1)] Division of Earth and Ecosystem Sciences
[(2)] Division of Atmospheric Sciences

Executive Summary

Introduction: This report provides information in support of the development of a Particulate Matter Reduction Plan (PMRP) for the Oceano Dunes State Vehicular Recreation Area (ODSVRA) by documenting the results of three Stage I-Pilot Projects: (1) the addition of artificial roughness to a sand surface (straw bale roughness demonstration plot); (2) establishment of a vegetation cover (vegetation effectiveness demonstration site): and (3) reduction or elimination of surface disturbance by driving of off-road vehicles (the vehicle exclosure transect).

Approach: The approach adopted in this study is based on the theoretical relationships (confirmed by numerous field studies) that sand transport rates and dust emissions scale as a power function of wind speed or wind friction speed. Reduction of sand flux therefore has a non-linear effect on dust emissions. Pilot projects 1 and 2 were based on field and laboratory wind tunnel studies, which have shown that significant reductions in sand transport rates occur as a result of the presence of non-erodible surface roughness elements, including vegetation and solid objects (cylinders, cubes, etc.). This is the result of two complimentary processes: 1) the partitioning of the wind shear stress between the surface and the roughness elements so that sand transport rates through areas of surface roughness are determined to a large extent by the roughness density λ (λ=n b h/ S, where n =number of roughness elements, b=element breadth, m, h=element height, m, and S is the area of the surface that contains all the elements), and 2) a roughness element height effect, where the taller the element the greater the enhancement provided by the roughness to reduce sand transport and the associated dust emissions.

Demonstration sites: The sand transport reduction effectiveness was measured and documented in projects 1 and 2 to assess their viability as long-term strategies for dust emissions reduction. Sand transport was measured at the straw bale and vegetation sites using a combination of sand traps and electronic sand flux sensors (Sensit).

The straw bale roughness demonstration plot consisted of a 100 m by 50 m area of gently undulating sand on which 210 straw bales were placed in a staggered array designed to achieve a roughness density (λ) of 0.022 and a target reduction in sand flux of 50% at the trailing edge of the roughness array. The plot was aligned with the long axis parallel to the prevailing sand transporting wind and instrumented with 24 Cox Sand Catchers and 6 BSNE sand traps, together with an anemometer and sand flux sensors. During the 18-day study period (April 15 – May 3, 2011) sand transport occurred on all days except April 20 and 23. A total of 14 sand transport events lasting several hours or more each provided sufficient mass in the traps to allow for estimation of the sand flux reduction due to the added straw bale roughness. This was accomplished by comparing the sand flux measured at the upwind and downwind edges of the array, normalized to the upwind sand flux to enable comparison of reduction factors between events. A modal sand flux reduction of 40 – 50% was measured by the Cox Sand Catchers and 60-70% was measured by the BSNE traps. These values are consistent with theory and prior experimental results (Fig. A). Significant sand deposition occurred within the straw bale array over the course of the pilot project and resulted in the development of shadow dunes in the lee of the bales. However, the overall effectiveness of the array for sand flux reduction did not appear to be impaired over the duration of the project.

The vegetation effectiveness demonstration site was designed to show that existing dune vegetation does indeed restrict sand transport, by comparison of sand flux between un-

vegetated and vegetated areas in an area of variably vegetated dunes and sand sheets northwest of Oso Flaco Lake. Vegetation cover (mainly lupine), determined using line intersect transects, averaged 37%, with a range from 66% to 25%. As a result, sand flux was reduced by as much as 90-95% within the first 50 m from the upwind boundary of the vegetated area, and 90 – 99% further downwind, as measured by the Cox Sand Catchers and BSNE traps, resulting in minimal sand flux in the open sand areas between the vegetation.

Restriction or elimination of surface disturbance by vehicle traffic represents a third potential control measure, based on the hypothesis that disturbance may increase sand transport and dust emissions relative to undisturbed areas under similar wind regimes. This hypothesis was tested by measuring dust emissions (for a given wind friction speed) using the DRI Portable In Situ Wind ERosion Laboratory (PI-SWERL) device -for an undisturbed and immediately adjacent disturbed (riding) area along a transect across part of the dunefield. The data on dust emissions potential for this transect indicate that the effect of restricted driving on dust emissions is not certain. There are indications that the undisturbed area emits dust at lower rates that the driving area, but the range of emission rates obtained overlaps to a considerable degree between undisturbed and disturbed areas.

Dust emission potential: The potential for emission of dust of PM_{10} (10 micron aerodynamic diameter) size ($\mu g\ m^{-2}\ s^{-1}$) and saltation activity (particle counts s^{-1}) as a function of wind (friction) speed was assessed at all locations using the PI-SWERL device. At all sites, dust emissions are highly correlated ($r^2 > 0.99$) with increasing wind friction speed and therefore with wind speed (Fig. B). Although the sand transport activity as measured by the PI-SWERL should only be considered as an indicator of sand movement (i.e., not necessarily analogous to sand flux measured with traditional methods), there is a strong correlation ($r > 0.9$) between sand movement and dust emissions at all sites. The variation in dust emission potential between sites for a given applied wind friction speed is small and not statistically meaningful. This is likely controlled in large part by the texture of the Oceano Dunes sediments (i.e., percent sand, silt, and clay) as texture of the top centimeter of sands at all test locations is similar and dominated by the sand fraction (99%). The silt- and clay-sized particles comprise 1% or less of the sediment in all test locations.

Conclusions: This study established that addition of roughness in the form of vegetation and/or artificial elements (e.g., straw bales) is an effective way to reduce sand movement, and the accompanying dust emissions at Oceano Dunes. The reduction in sediment transport is caused by the need for higher regional wind speeds to initiate dust emissions thus reducing the range of wind speeds that result in emission, and by partitioning of the available shear stress between the roughness elements and the surface. At the straw bale site, sand movement was reduced by approximately 57% compared to upwind values. Using the relationship between wind friction speed and dust emissions derived from the PI-SWERL testing in combination with theoretical and empirically-verified relationships between the density of roughness elements and the amount of regional wind shear stress that reaches the ground surface between the elements, we estimate that 48% of the regional shear stress reaches the intervening surface among the straw bales, which would result in a lowering of the PM_{10} emissions as a function of wind friction speed by ≈98% (for all friction speeds above the sand transport threshold), as compared with the surface in the absence of straw bale roughness. In addition, we estimate that the minimum wind velocity (at 10 m height) required to initiate sand transport at the straw bale site (≈7.9 m/sec) is higher than it is for bare sand (≈5.3 m/sec). Thus the overall PM_{10}

emissions will decrease because higher wind speeds will be required to activate the sand and dust transport system.

The vegetation pilot site has even greater potential to reduce PM_{10} emission compared to bare sand through the almost complete elimination of sand transport within this area. The roughness control method as tested in two configurations is a highly effective method for PM_{10} control and could form the basis for viable control strategies at Oceano Dunes. The effectiveness of restricted driving to reduce PM_{10} emissions is less certain than the clear results from the roughness demonstration projects. However, there was some indication that emissions of dust for the same wind speed were lower in the exclosure area than in the driving area. This difference was modest and less than factor of two.

Recommendations: Based on the pilot study results and reviewing some of the uncertainties that remain we have some recommendations for additional actions that could be pursued to provide better understanding of the Oceano Dunes dust emission system, which would allow better plans to be developed to control those emissions.

Currently the available data suggest that variability in PM_{10} emissions is limited at least across the pilot test areas, suggesting that controls applied in either of the three test locations would be equally valuable in reducing the overall PM_{10} emissions originating within these dune areas. To better determine if the observed variability is restricted or if the available data reflect a bias due to the small sample size, we recommend additional PI-SWERL measurements be made along transects from the high water line inland towards the eastern edge of the park. This will allow for the determination of the existence of high emitting areas, or whether variability in emissions lies within a restricted range, which will have an impact on the nature of any control strategies adopted.

Related to this is the continued uncertainty as to the relative sand transport and emission activity among different areas on the dunes. Although we can now be confident that the vegetated areas have low sand flux rates and low emission potential due to the roughness effect, there are only limited data available to judge the relative activity levels of sand movement in the driving area versus the exclosure area. We recommend that active monitoring of wind speed and direction and sand movement be considered for each area.

The availability of measured PM_{10} emission rates as a function of wind friction speed from the PI-SWERL measurements offers the opportunity to use dispersion modeling to evaluate how control measures could affect the downwind concentrations of PM_{10} outside the park. We recommend that to better inform the development of an overall control strategy a dispersion modeling exercise be undertaken to estimate how much area would need to be controlled at the dunes, given its known emission potential and wind climatology, to reach PM_{10} levels downwind of the dunes to meet air quality standards.

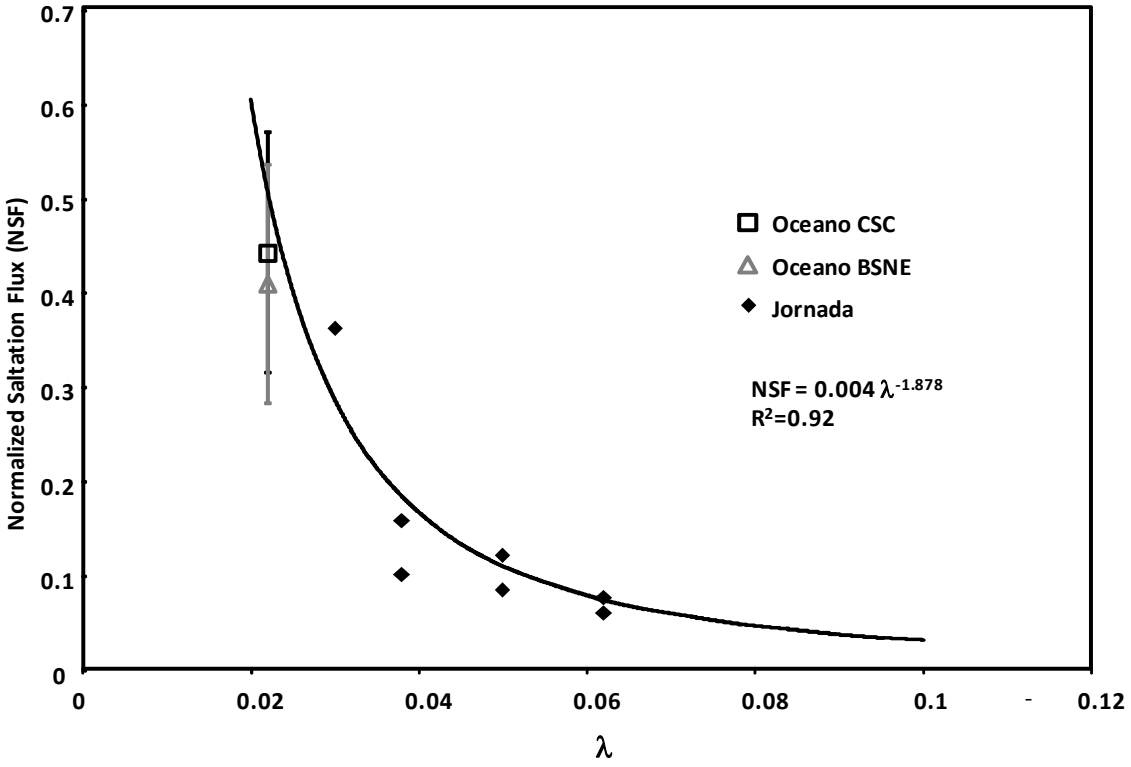

Figure A. Comparison of the normalized sand flux at the trailing edge of the straw bale roughness with data from a similar experiment carried out by Gillies et al. (2006) using 5 gallon-buckets as roughness elements at the USDA Jornada Experimental Range, New Mexico.

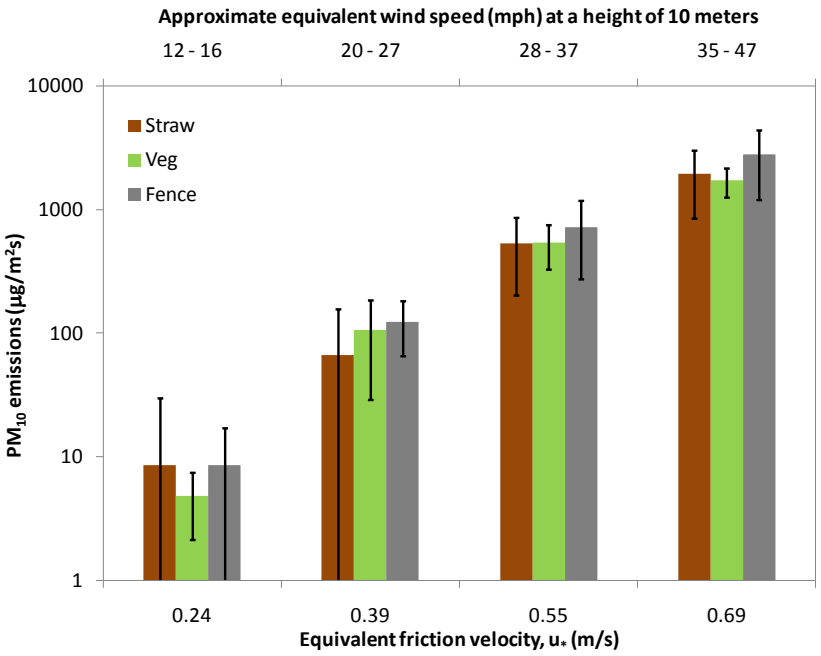

a. Comparison of PM_{10} dust emissions magnitudes across three locations

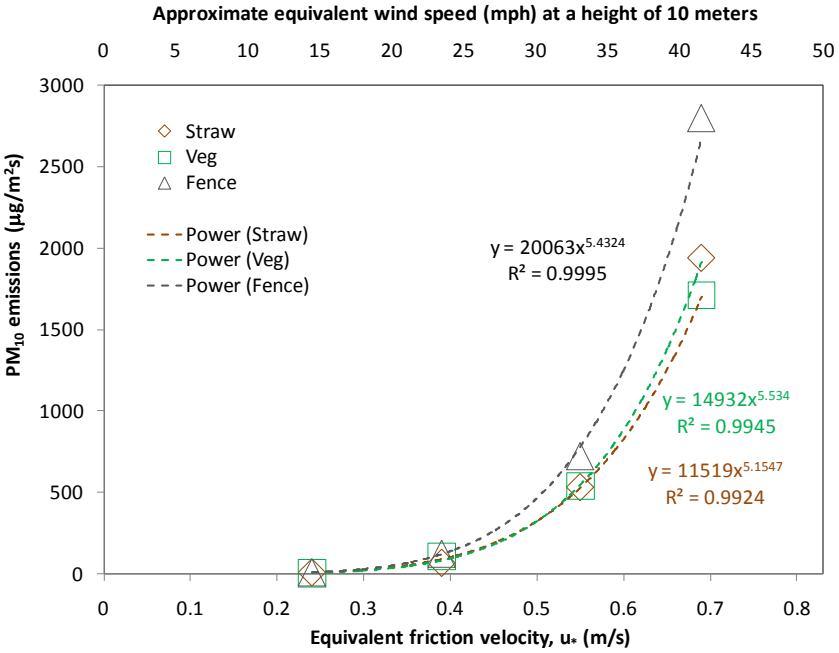

b. Power fits to PM_{10} dust emissions for measurements at three test locations

Figure B. Relative magnitudes of emissions from straw bale, vegetated, and along-fence measurements using combined data from both PI-SWERLs.

1. Introduction

This report provides information in support of the development of a Particulate Matter Reduction Plan (PMRP) for the Oceano Dunes State Vehicular Recreation Area (ODSVRA) by describing field studies of three Stage I-Pilot Projects. These pilot projects were small-scale sand flux control measures, whose emission reduction effectiveness were measured and documented to evaluate their viability as long-term strategies.

Control measures to reduce sand movement at Oceano Dunes are needed to provide for downwind reductions in emissions of particulate matter ≤10 µm aerodynamic diameter (i.e., PM_{10}), which is a U.S. EPA regulated air pollutant under the Clean Air Act. Based on prior studies that show a correlation between sand movement in the dune area and elevated downwind PM_{10} emissions (Craig et al., 2010), this project was designed to evaluate several methods to achieve sand flux reduction leading to reduced PM_{10} emissions. The measurement strategy also offered the opportunity to evaluate whether the test areas differed significantly in their PM_{10} emission potential or if the variability in this potential was limited. This latter information was deemed to be useful to evaluate whether highly emissive areas could be remediated to achieve lower downwind levels or for the case of relatively consistent emission potential over wide areas, the remediation actions would require reducing the total extent of the areas that are emissive.

Control measures should be scientifically defensible, logistically feasible, and cost effective. Pilot projects are needed to demonstrate the degree of sand flux reduction as well as the logistical feasibility of proposed control measures. They should provide significant reduction in sand flux and therefore PM_{10} emissions, based on correlations between wind strength and sand movement in the Pilot Project area and PM_{10} emission potential determined using the Portable In-Situ Wind Erosion Laboratory (PI-SWERL) device (*Etyemezian et al*., 2007).

Following extensive discussions with California State Parks (CSP) and San Luis Obispo County Air Pollution Control District (SLOCAPCD) personnel in January and February 2011, three pilot projects were selected for further study of their effects on reducing sand transport and dust emissions: (1) the addition of artificial roughness to a sand surface; (2) establishment of a vegetation cover: and (3) reduction or elimination of surface disturbance by driving of off-road vehicles.

2. Conceptual background for pilot projects

Recent conceptual advances together with field and laboratory wind tunnel studies show that significant reductions in sand transport rates occur as a result of the existence of surface roughness elements, including vegetation and solid objects (cylinders, cubes, etc.). This is the result of the partitioning of the wind shear stress between the surface and the roughness elements and the interaction of the moving sand with the elements (*Gillies et al*., 2006).

When the wind blows over a smooth unobstructed surface, the total force of the wind F (N) is imparted more or less uniformly across the entire surface. The shear stress τ (N m^{-2}) per unit area A_S (m^2) of the surface is defined by:

$$\tau = F/A_S \quad (1)$$

In the case of surfaces covered with large roughness elements, the total frictional force imparted to the surface is equal to the sum of the frictional forces on the roughness elements F_r and the intervening surface F_g so that:

$$F = F_r + F_g \quad (2)$$

A proportion of the shear stress is absorbed by the elements protecting the intervening erodible surface. The degree of protection created by the partitioning of the shear stress is a function of the size, geometry, and spacing of the elements and can be expressed by the ratio between the threshold wind friction speed with and without roughness elements *(Raupach et al., 1993).*

$$R_t = \frac{1}{(1 - m\sigma\lambda)^{0.5}(1 + m\beta\lambda)^{0.5}} \quad (3)$$

where: R_t = threshold wind friction speed (or shear stress) ratio

σ = roughness element basal area to frontal area ratio

λ = roughness density

β = ratio of element to surface drag coefficients

m = an empirical constant

As indicated above, the presence of surface roughness elements increases the threshold wind friction speed for sediment transport. In turn, this affects the overall magnitude of sand transport.

This approach has been shown to have wide applicability for understanding the effect of vegetation or solid roughness elements on boundary layer winds and sediment transport in field and laboratory experiments *(Crawley and Nickling, 2003; Gillies et al., 2007; Gillies et al., 2006; King et al., 2006; Wolfe and Nickling 1996)*. Knowledge of the effect of roughness on sand transport can also be used to determine the amount of roughness necessary to reduce sand transport to selected levels.

Addition of artificial roughness elements

Field and wind tunnel testing have indicated that aeolian sediment transport rates through areas of surface roughness are determined to a large extent by the roughness density λ (λ=n b h/ S, where n =number of roughness elements, b=element breadth, m, h=element height, m, and S is the area of the surface that contains all the elements) (e.g., *Lancaster and Baas, 1998*; *Gillies et al., 2006*). The data presented by *Gillies et al*. (2006) show that knowledge of the roughness density of a surface can be used to predict the effect roughness has on reducing sand flux compared with a similar surface in the absence of non-erodible roughness elements. However, they noted that element size plays an important role in influencing the magnitude of the reduction that cannot be accounted for based solely on knowledge of λ. When the dimensions of the roughness itself are equivalent to the full range of saltation length units (particle hop length and hop height) it appears that additional effects, caused by the interaction of the elements with the saltation cloud, reduce the transport efficiency to a much greater extent than for surfaces with smaller roughness elements of equivalent roughness density. The effect of large and small elements having the same roughness density on saltation flux is shown in Fig. 1.

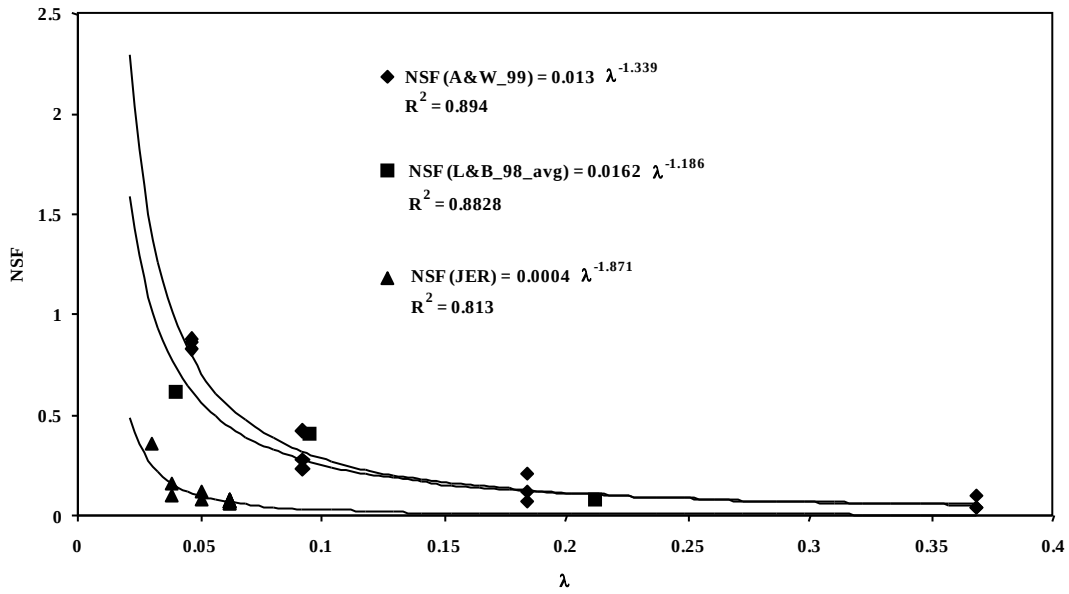

Figure 1. Comparison between the measured normalized saltation flux (NSF) as a function of λ from *Al-Awadhi and Willetts* [1999] (small cylinders, black diamonds), *Lancaster and Baas* [1998] (saltgrass, black squares), and the data of *Gillies et al*. [2006] for large roughness elements (5 gallon buckets, represented by the black triangles). Normalized saltation flux (NSF) is defined as sand flux exiting/sand flux entering the roughness array.

Because it is logistically unfeasible and scientifically challenging to directly measure PM_{10} emission reductions as a result of pilot project implementation, we proposed to: (1) determine the degree of sand flux reduction as a result of control measures, and (2) measure emission potential in the control areas using the PI-SWERL; and (3) to infer the degree of PM_{10} emissions reduction by modeling relationships between wind speed and PM_{10} emission potential measured in the field by the PI-SWERL, for the Pilot Project areas.

Sand flux reduction as a result of pilot project implementation can be determined following the control area concept, by measuring the influx and outflux of sand. The sand flux reduction factor can be calculated as:

$$\frac{Sand\ influx - Sand\ outflux}{Sand\ influx} \quad (4)$$

Additional sand flux measurements within the control area are required to determine the distance over which sand flux is reduced to a new equilibrium value. Such measurements are important to verify that all the sand flux reduction takes place within the control area and to provide information that can be used to determine the size and geometry of full-scale control measures.

3. Pilot Project Location and Site Characteristics

The implemented Pilot Projects were as follows: (1) the straw bale roughness demonstration plot, (2) the vegetation effectiveness demonstration site, and (3) the vehicle exclosure transect. Figure 2 shows the location of the three Pilot Projects.

Figure 2. Location of the three pilot projects. Riding area delineated by red line.

3.1 Straw Bale roughness demonstration plot

This potential control measure was based on recent conceptual advances together with field and laboratory wind tunnel studies that show that significant reductions in sand transport rates occur as a result of the existence of surface roughness elements, including vegetation and solid objects (cylinders, cubes, etc.). This is the result of the partitioning of the wind shear stress between the surface and the roughness elements and the interaction of the moving sand with the roughness. DRI personnel supervised California State Parks personnel in the placing of straw bales in a 100 m by 50 m area located immediately north of the S1 wind tower. The long axis of the array was parallel to the dominant sand transporting wind direction (300° magnetic). Straw bales (each with dimensions of approximately 1.17m long by 0.4 high by 0.6 m wide) were placed in a staggered array consisting of 20 alternating rows of 10 and 11 bales each. Center to center spacing of the bales in each row was 4.9 m, and the rows were spaced 4.9 m apart (Fig. 3). The designed sand flux reduction was 50% (i.e., NSF=0.5), based on the results of *Gillies et al*. (2006).

Figure 3. Straw Bale Roughness Demonstration Plot – view to southeast and S1 tower.

3.2 Vegetation effectiveness demonstration site

Field studies show that sand flux is reduced significantly in areas that are vegetated, as a result of surface protection and shear stress partitioning in a similar way to the roughness elements described above (*Musick and Gillette*, 1990; *Okin*, 2008; *Wolfe and Nickling*, 1993).

In the case of the Oceano Dunes, environmental restoration efforts show that establishment of a dense vegetation cover is achievable. It was however, not feasible to establish a vegetation control area in the available time, so the alternative as a pilot project was to demonstrate that existing dune vegetation does indeed restrict sand transport. A suitable area of vegetation was instrumented to measure sand flux and transport thresholds for direct comparison with an adjacent un-vegetated sand area. Comparison of sand flux between the un-vegetated and vegetated areas provided a sand flux reduction factor for the studied vegetation type and cover. In consultation with California State Parks staff, an area of variably vegetated dunes and sand sheets (Fig. 4) adjacent to Oso Flaco Lake was selected for this experiment. The site was located in a re-vegetated trough between the arms of two parabolic dunes, each approximately 8 m high. The trough sloped gently up to the southeast. To the northwest is an area of active 3-4 m high crescentic dunes that appear to be migrating into the vegetated area.

Figure 4. Vegetation effectiveness demonstration site – view to SE.

3.3 Vehicle exclosure transect

This potential control measure relies on the hypothesis that surface disturbance by vehicles increases sand transport and dust emissions relative to undisturbed areas under similar wind regimes. This hypothesis was tested by measuring dust emissions (for a given sand wind friction speed and sand transport rate) using the PI-SWERL for an undisturbed and immediately adjacent disturbed (riding) area. If emission factors and sand transport rates for undisturbed and disturbed areas are not significantly different, then restricting vehicle access will have no effect on sand flux and emissions. If, however, there is a statistically significant difference, then restricting access could be a viable control measure.

Measurements of sand transport and dust emissions were made using the DRI PI-SWERL device along a transect on each side of the fence separating the riding area from an area that has not been accessible to vehicles for many years (Fig. 5).

Figure 5. View of area of vehicle exclosure transect from exclusion area (foreground) SW towards riding area (middle distance).

4. Data Collection

Following delays due to bad weather and DRI personnel commitments, the three pilot projects were set up and instrumented in the period April 12 – 15, 2011. For projects (1) and (2), instruments were maintained and measurements of sand flux made for the period April 15 to May 4, 2011. For project (3), all necessary measurements were made on April 14.

4.1 Instrumentation

4.1.1. Straw bale roughness demonstration plot

The straw bale site was instrumented with 24 Cox Sand Catchers (CSC) placed in 6 rows of 4 traps, beginning immediately upwind of the first row of straw bales (A) and then in the center of the lane between straw bale rows 4 and 5 (B); 8 and 9 (C); 12 and 13 (D); 16 and 17 (E), and 18 and 19 (F). BSNE (Big Springs Number Eight) sand traps (*Fryrear*, 1986) were also installed in the center of each of the rows of Cox Sand Catchers. The height of the inlet for all traps was set at 15 cm, and adjusted daily to account for changes in sand surface elevation.

A Sensit sand flux sensor was co-located with the BSNE trap on row A (upwind) and with the 2.2 m anemometer/wind direction mast located in the center of the array between straw bale rows 14 and 15. The height of the sand flux sensor was set at 15 cm, the same as the sand trap inlet. Instrument locations are shown in Fig. 6.

4.1.2 Vegetation effectiveness demonstration site

Instruments were placed as follows (Fig. 7): (1) an anemometer and wind direction sensor (at 2 m height), Sensit, Cox Sand Catcher, and BSNE trap were co-located upwind in an area of un-vegetated sand sheet to measure the sand flux in the absence of vegetation (A); (2) Cox Sand Catchers and BSNE sand traps were placed in open sand areas between vegetation at distances of up to 150 m from the upwind edge of the vegetated area. An additional Sensit was co-located with a BSNE trap (D) within the vegetated area. The height of the inlet for all traps was set at 15 cm, and adjusted daily to account for changes in sand surface elevation. The height of the sand flux sensors was set at 15 cm, the same as the sand trap inlet.

4.1.3 PM_{10} Emission Potential Measurements with PI-SWERL

The PI-SWERL measurements were conducted at three separate locations. At all locations, two PI-SWERLs (labeled “Black” and “Brown”) were operated at the same time. On April 13, 2011, the PI-SWERLs were operated at the straw bale roughness demonstration plot where the straw bales were slated to be installed the following day. These measurements were intended to provide a baseline for the PM_{10} emission potential of the sand prior to placement of the roughness elements.

Later on April 13, the PI-SWERLs were operated at the vegetation effectiveness demonstration site where the dunes had been stabilized by the planting of vegetation. The purpose of these measurements was to determine if the process of stabilization had also resulted in a significant difference in the sands PM_{10} emission potential as compared with sand upwind of the site.

On April 14, 2011, the two PI-SWERLs were operated side-by-side along the fence of an exclosure that was emplaced to restrict access to off-highway vehicles. The black PI-SWERL was operated on the side of the fence where recreational vehicles were permitted to operate, while the brown PI-SWERL was operated within the exclosure. Measurements were conducted about 20 - 30 m away from the fence whenever possible. The fence straddled a ridge, which was generally steeper on the inside of the exclosure than the outside. In some instances, it was

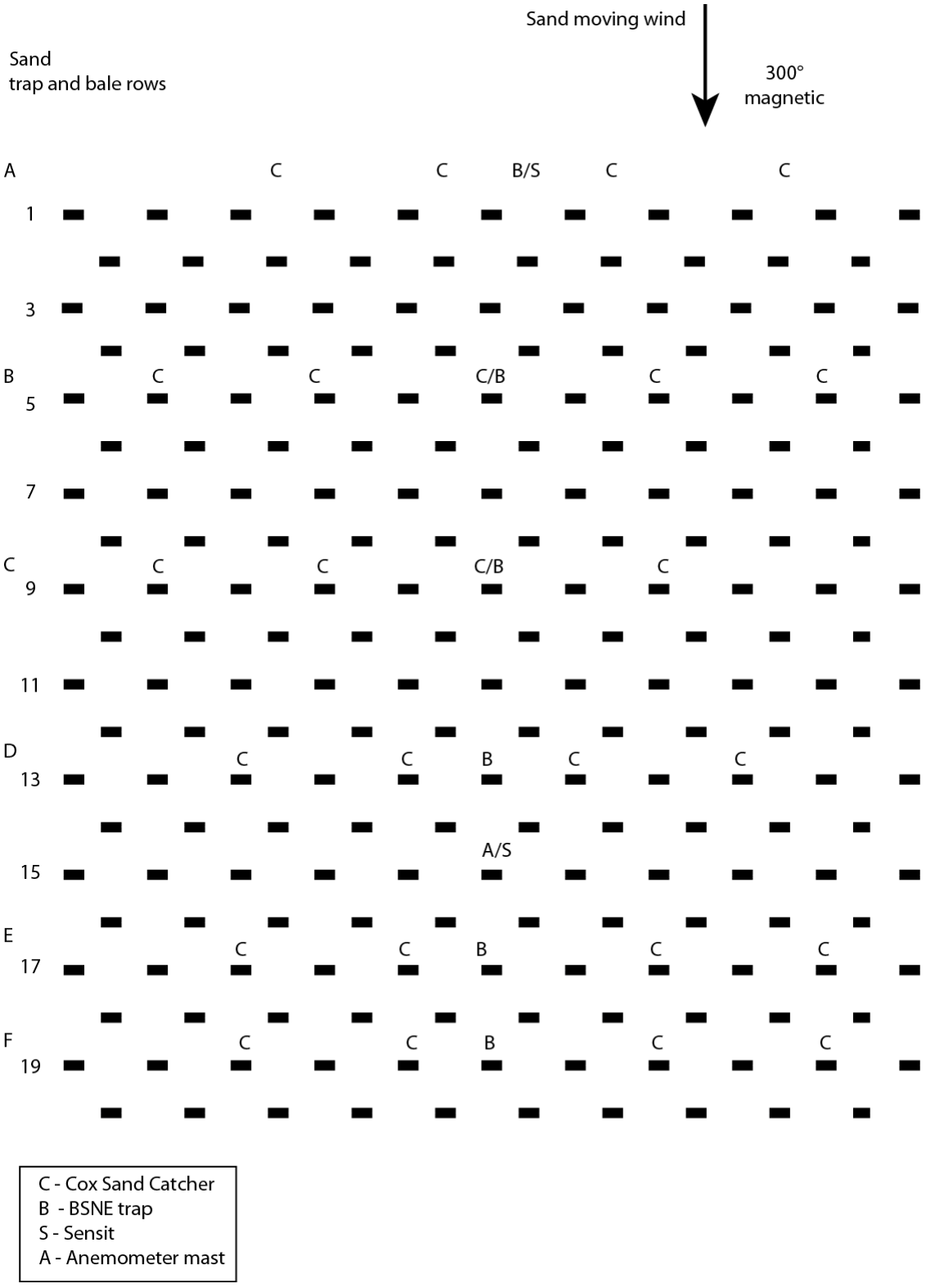

Figure 6. Layout of instrumentation at straw bale roughness demonstration plot.

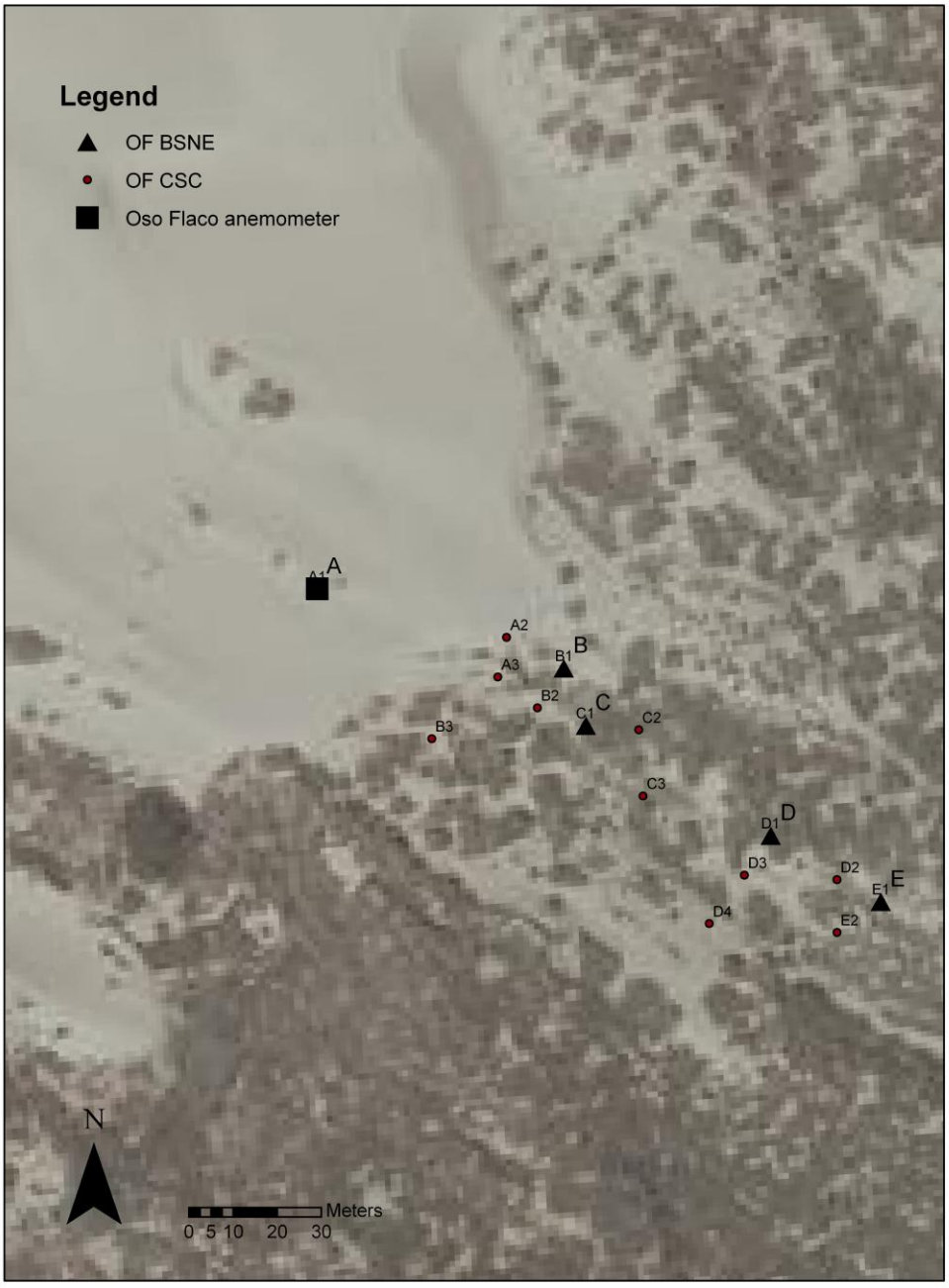

Figure 7. Location of instruments at vegetation effectiveness demonstration site.

necessary to conduct measurements as close as 2 m to the fence in order to sample the same dune with both PI-SWERLs. The fence and the measurements along it were initially oriented along the east/west direction, but then turned along the north south direction. The number of tests conducted at each location is shown in Table 1 and the GPS coordinates of each valid measurement are shown in Fig. 8.

In addition to the emission potential measurements, samples of the sand were collected to characterize the moisture content of the sediment and the particle size distribution. Sand samples were collected by removing sand to a depth of <5 mm around the perimeter of the PI-SWERL at its test position. The sand was placed in a Ziploc bag and returned to DRI for analysis. A total of 68 sediment samples were collected in association with PI-SWERL tests.

Table 1. Locations, times, and numbers of PI-SWERL measurements.

Test location	**Date and Time**	**Black PI-SWERL Valid # Tests**	**Brown PI-SWERL Valid # Tests**
Straw bale roughness demonstration plot	4/13/11 8:45 - 12:42	19	15
Vegetation effectiveness demonstration site	4/13/11 14:07 - 17:24	7	14
Vehicle exclosure transect	4/14/11 8:20 - 13:00	18	18

5. Data analysis

5.1 Sand Flux

Sand flux was calculated as follows: the mass of sand collected each day in each BSNE trap and CSC was divided by the fraction of the time during that day that the upwind Sensit was recording sand movement to obtain a transport rate in gm/m^2 hr.

The effectiveness of the array of straw bales was assessed by comparing the sand flux measured at the upwind and downwind margins of the plot, using the control area approach. The sand flux reduction factor was calculated using Eq. 4. The sand flux reduction factor was calculated separately for the BSNE traps and the Cox Sand Catchers.

For the Straw Bale Roughness demonstration plot, the sand flux for the BSNE trap A and the mean sand flux of row A of the CSCs was taken as the upwind or influx sand transport rate. The sand flux for the BSNE trap F and the mean sand flux of row F of the CSCs was taken as the downwind or out-flux sand transport rate.

For the Vegetation Effectiveness Demonstration site, the upwind or influx sand transport rate was defined by BSNE trap A and Cox Sand Catcher A1, co-located with Sensit C and the anemometer mast. The downwind or out-flux was defined by BSNE trap E and Cox Sand Catcher row E.

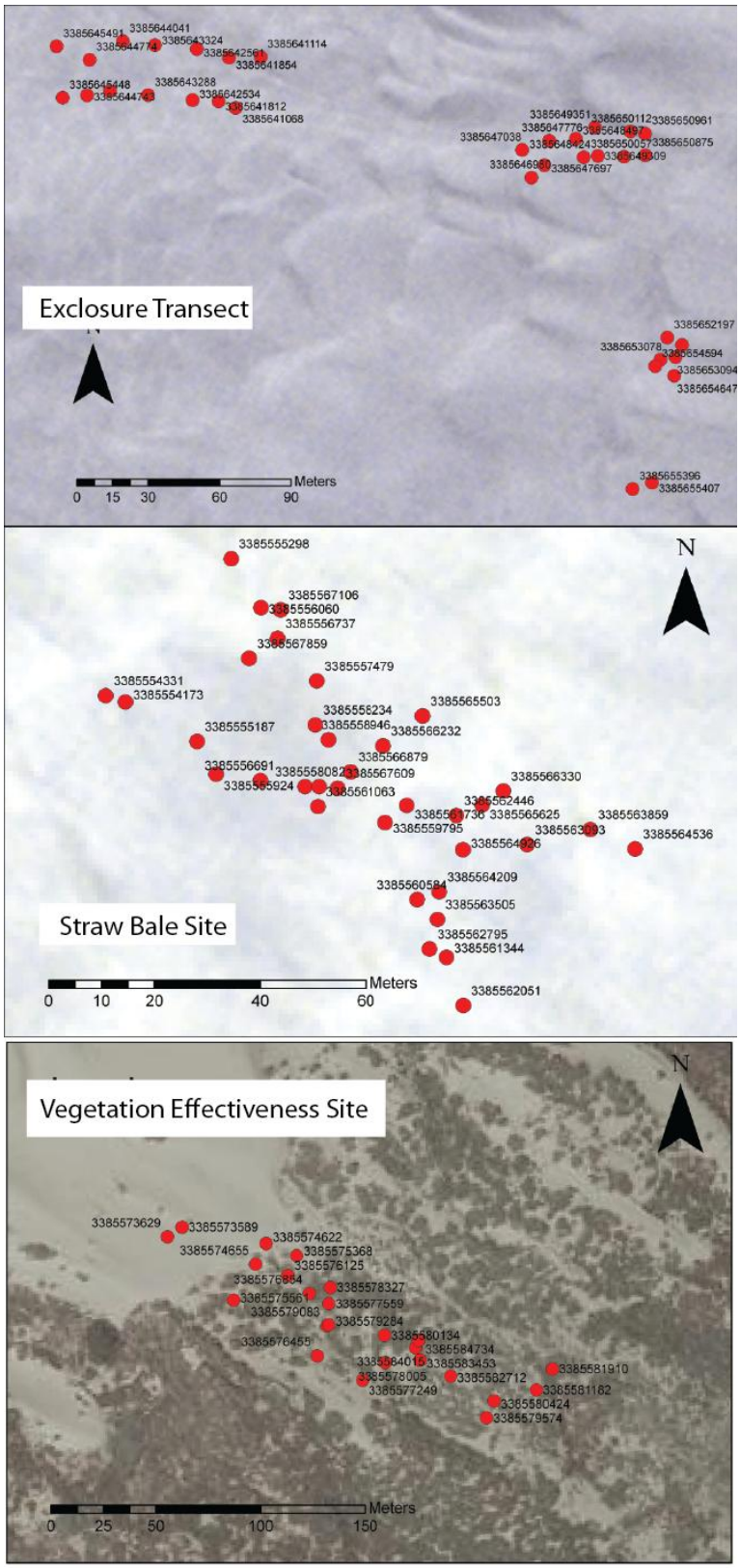

Figure 8. Locations of PI-SWERL measurements. Dashed black and brown arrows represent approximate direction of travel during testing.

5.2 PM_{10} Dust Emission Potential

A typical PI-SWERL measurement at the Oceano Dunes is shown in Fig. 9. The measurement cycle consisted of an initial clean air flush (60 seconds), a short ramp to 1000 RPM (30 seconds), maintain 1000 RPM (55 seconds), ramp up to 2000 RPM (60 seconds), maintain 2000 RPM (60 seconds), ramp up to 3000 RPM (60 seconds), maintain 3000 RPM (90 seconds), ramp up to 4000 RPM (60 seconds), maintain 4000 RPM (90 seconds), and turn of blade motor and proceed with final clean air flush (60 seconds). The example in Fig. 9 shows that the clean air blower flow-rate was steady at 100 liters per minute (lpm) and that the actual PI-SWERL blade's rate of revolution (RPM) very closely followed the target rate (TRPM). It would appear from the DustTrak PM_{10} concentration measurements that dust emissions begin at around RPM 1500, but this is not necessarily true. It is possible that dust emissions started earlier (e.g., RPM =1000), but that when graphed along the very high PM_{10} concentrations that result at RPM = 4000, those smaller values of concentration cannot be discerned. Another item of note on the figure is that two of the four optical gate sensors (OGS) begin to exhibit saturation behavior after the 3000 RPM step. This is a result of the very large sand fluxes on the types of dune surfaces sampled. Due to subtle differences in how OGS sensors are oriented within the PI-SWERL chamber, some may become saturated while others may remain below the saturation limit (about 280 counts per second). The majority of measurements conducted with both PI-SWERL units exhibited this type of saturation behavior for the two OGS sensors located near the surface. This was true on both days of testing and at all of the pilot project locations. The two OGS sensors that are located at a higher location within the PI-SWERL chamber (about 15 cm off the test surface) were less prone, but not immune to saturation behavior. Data from those sensors have been used in subsequent data analysis since they do provide an indication of sand movement within the PI-SWERL. Higher OGS counts (up to the saturation limit of about 280 counts per second) are indicative of more vigorous sand movement within the PI-SWERL. However, sand movement as measured by these OGS sensors, which are elevated above the test surface, cannot be easily related to a traditional measure of sand flux (e.g., by sand catcher).

Dust emissions at specific values of RPM were calculated by averaging the one-second dust emissions over the intervals shown in Fig. 9, which were calculated as:

$$E_i = \left(C_{DT,i} \times F_i/60\right)/A_{eff} \quad (5)$$

where E_i = PM_{10} dust emissions in units of μg/m^3 at the i^{th} second into the measurement cycle, $C_{DT,I}$ = the DustTrak –measured PM_{10} in mg/m^3 at the i^{th} second, F_i = the clean air flow rate in (and out) the PI-SWERL chamber in liters per minute at the i^{th} second, and A_{eff} = the effective area of influence of the PI-SWERL annular blade and is equal to 0.026 m^2.

Similarly, count values from the optical gate sensors (OGS) where averaged over the periods indicated in Fig. 9. However, OGS averages exceeding 250 counts per second were not considered valid and do not appear in later data presentation.

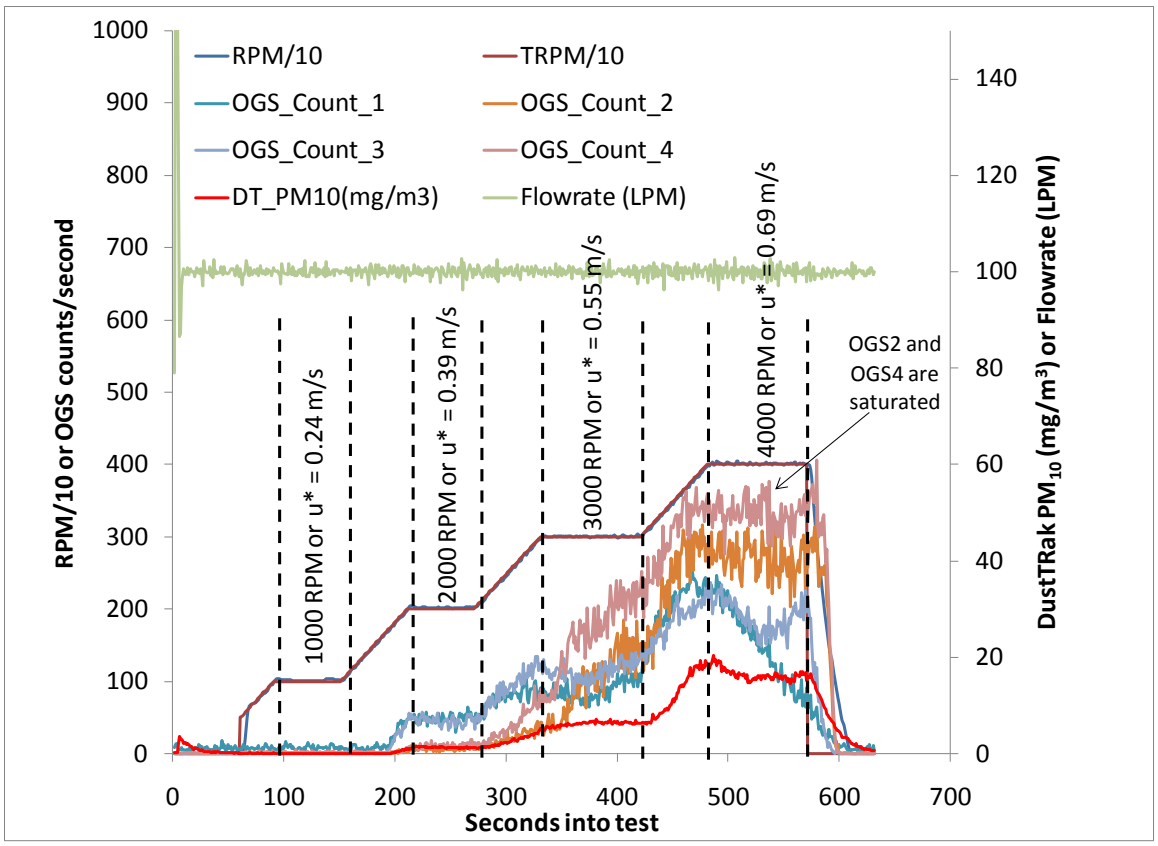

Figure 9. Example PI-SWERL measurement from Oceano Dunes. Vertical lines indicate periods when RPM were held constant and the equivalent smooth surface wind friction speed.

On the second day of testing (4/14/11) it was noted that the DustTrak being used in conjunction with the black PI-SWERL appeared to be reporting unduly high concentrations of PM_{10}. This was confirmed when the DustTraks were switched between the black and brown PI-SWERLs for the last five pairs of measurements along the fence; after the switch, PM_{10} concentrations from the brown PI-SWERL were unduly high compared to the black PI-SWERL. This discrepancy between DustTraks was not observed on the first day of testing. Prior to the field measurements, collocation of the two DustTraks indicated that DT2 (used with black PI-SWERL) would need to be multiplied by 0.88 in order to obtain the same value that DT1 (used with the brown PI-SWERL) reports, essentially within the manufacturer's guidelines of 10% inter-instrument variation. This level of instrument variation is considered acceptable and generally does not warrant applying any corrections to the data.

Following the field measurements, the two DustTrak were collocated at the DRI laboratory in Las Vegas. Samples of Oceano Dune sand were placed on a hard surface and a PI-SWERL was operated on the surface. The two DustTraks were connected to the PI-SWERL exhaust and the data streams from both units were logged in unison. As Fig. 10 clearly shows, the DustTrak that was used primarily in conjunction with the black PI-SWERL was under-

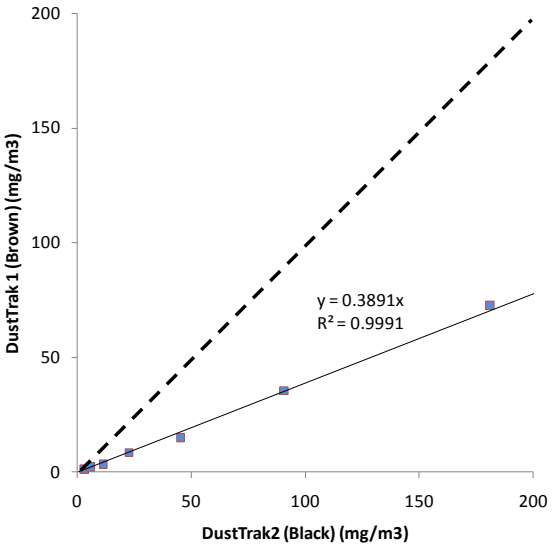

Figure 10. Laboratory comparison of response of DustTraks used on black and brown PI-SWERL unit following the transect measurements.

reporting by a factor of 2.6 (1/0.389) compared to the DustTrak that was used primarily in conjunction with the brown PI-SWERL. We hypothesize that during the act of cleaning the instrument in between testing days, the DustTrak that accompanied the black PI-SWERL somehow went out of calibration. This much higher level of instrument variation is not small and some correction must be applied to the DT2 concentrations. In order to compare data from the black and brown PI-SWERLs, the DustTrak concentrations measured by DT2 (black PI-SWERL except last five tests on 4/14/11) were multiplied by 0.389 for data collected on 4/14/11. Since applying a correction was necessary for data collected on 4/14/11, a correction was also applied for data collected on 4/13/11 for consistency in data analysis. Specifically, concentrations measured by DT2 were multiplied by 0.88 for data collected on 4/13/11.

5.3 Particle Size Distribution Measurements

A set of sand samples representing the three pilot project locations (10 straw bale samples, 5 vegetation samples, 4 ATV driving samples, and 6 from within the driving exclosure area) were submitted for particle size analysis to the DRI Soil Characterization Laboratory in Reno, NV. The samples were characterized for determination of their particle size distributions in the sand fraction for five size ranges: 2.0-1.0 mm, 1.0-0.5 mm, 0.5-0.25 mm, 0.25-0.125 mm, and 0.125-0.0625 mm. The percent sand, silt, and clay were also estimated. Analysis was done with a high resolution Micromeritics Saturn DigiSizer 5200 laser particle size analyzer and auto-sampler.

5.4 Soil Moisture Measurements

The moisture content of the sand samples was determined in conjunction with the particle size analyses. The range of moisture content was 0 to 0.006 (g/g). The average percent moisture content was 0.07% (±0.001%). The very low moisture content of the surface sand material essentially negates a role for moisture to affect sand transport and dust emissions and the small range of values precludes developing a relationship to account for a moisture content effect.

6. Data Sets

6.1 Sand flux and Wind Measurements

Measurements of wind speed and direction, Sensit sand saltation intensity, and sand transport were conducted during the period April 15 – May 4, 2011 for the straw bale roughness demonstration plot and the vegetation effectiveness demonstration site.

Wind speed and direction were sampled every second and compiled into 1 minute, 10 minute, and hourly averaged values of wind speed and direction. Wind data were subjected to standard QA/QC procedures by EMC, Paso Robles. Figure 11 shows the time series of hourly wind speed at the straw bale roughness demonstration plot and the vegetation effectiveness demonstration sites. Winds at both sites were very similar in magnitude and frequency at both locations, and closely correlated ($r^2 = 0.89$). In addition, the wind speed measured by the anemometer at the straw bale roughness demonstration plot was very similar to that measured at the ST1 tower at the same height. The wind direction sensor at the straw bale site unfortunately failed soon after installation, so wind direction was determined using the 2 m anemometer at the ST1 tower.

At the straw bale roughness demonstration plot, sand transport occurred on all days of this period except April 20 (when rain occurred) and April 23. On the remaining days, very low values of sand transport were measured on April 18, 19, 24, and May 1, 2, and 4. A total of 12 significant sand transport events, (defined as periods in which measured sand collected in the upwind traps exceeded 10 gm) lasting several hours or more each were available for estimation of the sand flux reduction due to the added straw bale roughness (Table 2). Most of these events occurred on days when the 24hr mean PM_{10} concentration exceeded 50 $\mu g\ m^{-3}$ at the CDF monitoring site (Table 2). At the vegetation effectiveness demonstration site, sand transport occurred on the upwind sand sheet on all but three of the pilot project days. A total of 14 significant sand transport events (defined as above), each lasting several hours or more, occurred at this location (Table 2). Figure 12 shows the time series of sand flux for both sites; sand flux is generally much higher at the straw bale roughness demonstration plot, compared to the vegetation effectiveness site.

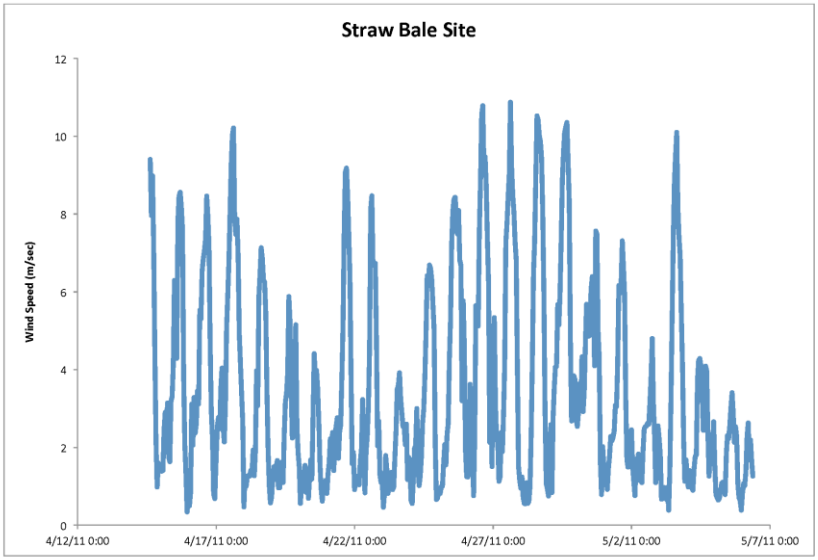

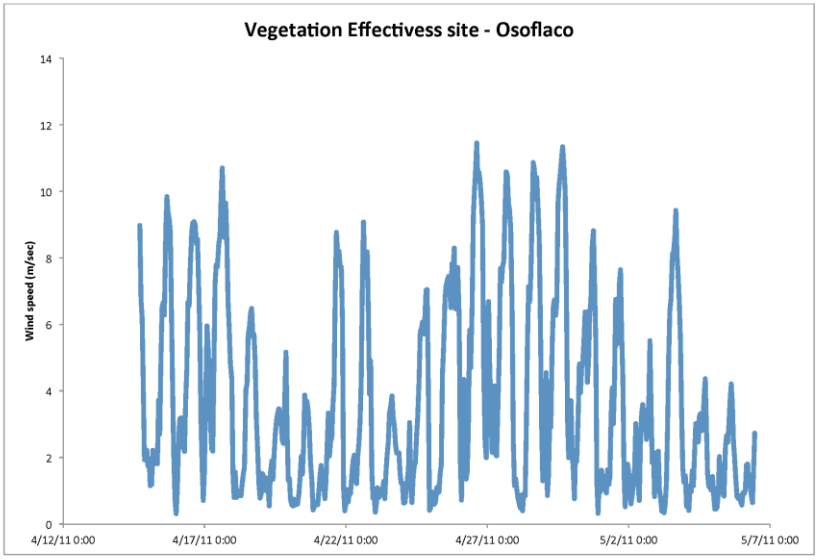

Figure 11. Time series of hourly wind speed at straw bale and vegetation study sites.

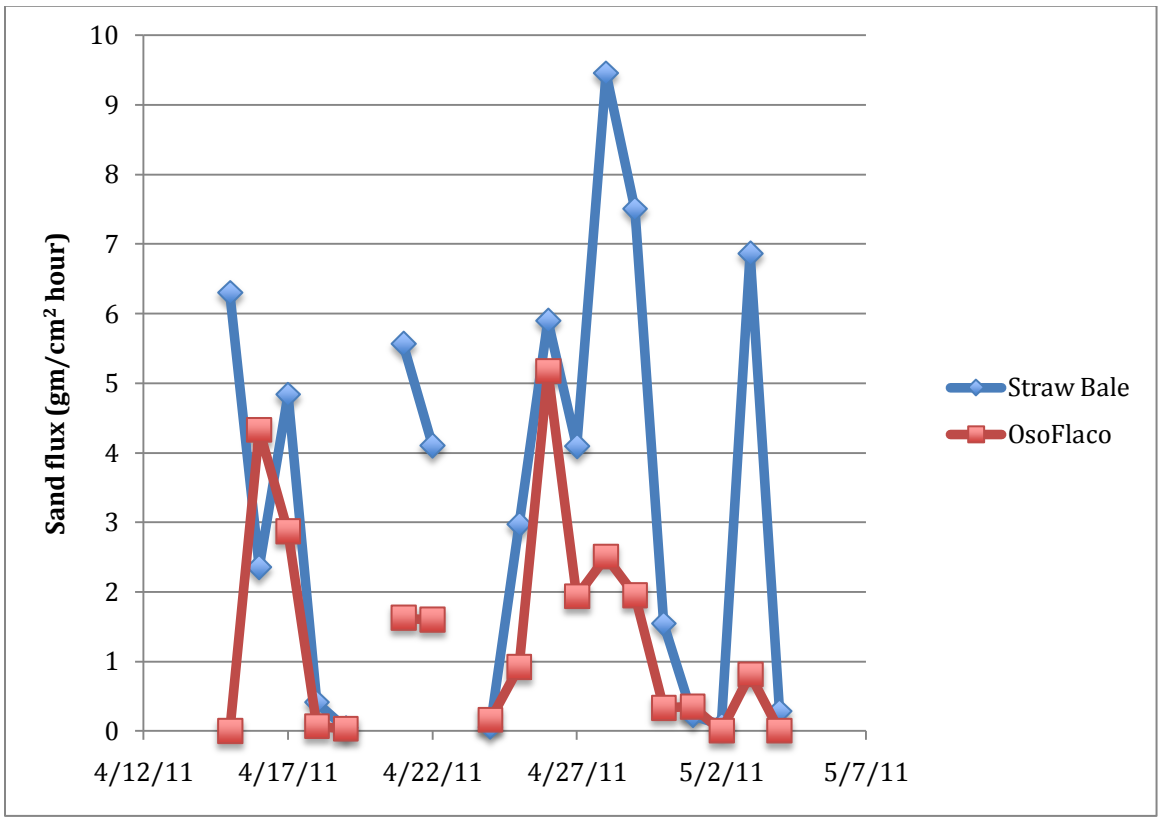

Figure 12. Time series of sand flux (daily mean) at the Straw Bale and Vegetation Effectiveness sites; data from upwind BSNE traps.

Table 2. Duration of Sand Transport Events (Highlighted periods provided sufficient data for estimation of sand flux reduction effectiveness).

STRAW BALE				10 m ST1 Wind direction (degrees)	CDF 24 hr PM_{10}	VEGETATION EFFECTIVENESS		
Date	Start	End	Duration			Start	End	Duration
15-Apr	**12:35**	**18:00**	**5:25**	298	94	13:20	18:35	5:15
16-Apr	**9:55**	**17:25**	**7:30**	298	104	**7:50**	**18:35**	**10:45**
17-Apr	**8:35**	**17:50**	**9:15**	297	92	**6:45**	**19:35**	**12:50**
18-Apr	11:45	16:20	4:35	284	25	10:30	17:40	7:10
21-Apr	**13:00**	**18:30**	**5:30**	262	51	**12:55**	**19:25**	**6:30**
22-Apr	**12:10**	**16:30**	**4:20**	290	52	**11:55**	**18:10**	**6:15**
25-Apr	9:50	18:30	8:40	287	66	**8:20**	**22:40**	**14:20**
26-Apr	10:05	18:40	8:35		140	**6:50**	**7:45**	**0:55**
26-Apr						**8:30**	**19:05**	**10:35**
26-Apr						**22:45**	**23:40**	**0:55**
27-Apr	**9:00**	**18:45**	**9:45**	298	122	**8:40**	**19:10**	**10:30**
28-Apr	**9:15**	**18:35**	**9:20**	293	131	**8:45**	**19:20**	**10:35**
29-Apr	**6:05**	**7:05**	**1:00**			**4:40**	**17:35**	**12:55**
29-Apr	**8:10**	**17:00**	**8:50**	306	128			
30-Apr	**6:45**	**8:10**	**1:25**					
30-Apr	**10:15**	**16:55**	**6:40**	300	44	**5:55**	**18:20**	**12:25**
1-May	**13:20**	**16:25**	**3:05**	286	56	10:25	16:40	6:15
3-May	**9:55**	**16:55**	**7:00**	291	103	0:00	21:00	21:00
3-May						22:15	23:55	1:40

7. RESULTS

7.1 Reduction of Sand Flux

7.1.1 Straw bale roughness demonstration plot

Table 3 shows the sand flux reduction factors for the major sand transport events. The modal reduction was 40 – 50% as measured by the Cox Sand Catchers and 60-70% as measured by the BSNE traps. The measurements for both types of trap are similar and closely correlated (r^2 = 0.70).

Some of the range can be attributed to the natural variability of sand transport in relation to the position of the sand traps (e.g., sand traps impacted by sand tails extending downwind from the straw bales), as well as to measurement errors inherent in the sand traps. There was no evidence for any relationship between the sand flux reduction and wind direction, although the range of wind directions measured during sand transport events was rather small (261° – 303°). There is some evidence to suggest that the sand-trapping effectiveness of the straw bale array was higher in the first two days after it was installed – giving rise to sand flux reduction factors of 75-84%, before falling to 40-50%. The time series of sand flux reduction factors is shown in Fig. 13. Mean values of the sand flux reduction factor are 55% and 57% for the CSC and BSNE, respectively. The reduction factors for May 3, 2011 are rather high (78 and 92% for the CSC and BSNE respectively) and these points appear to be anomalous outliers, perhaps because the wind direction for this day was from a more westerly direction (291°) compared to previous sand transport events (see also Table 2).

Air quality monitoring data (Craig et al., 20101) and Table 2 suggest that high levels of PM_{10} are associated with strong wind events. It is therefore useful to examine the relationships between the sand flux reduction factors and the overall magnitude of the sand transport events, as measured by the total Sensit count for each event. As Fig. 14 shows, there is no discernable relationship between the sand flux reduction and event magnitude, suggesting that the array of straw bales is similarly effective over a wide range of wind speeds.

7.1.2 Comparison to predicted sand flux reduction values

Based on the available data from *Gillies et al*. (2006), the reduction in sand transport resulting from the presence of large roughness elements can be estimated. The roughness density (λ) for the array as constructed was initially 0.22 – which was predicted to result in a 50% reduction in sand transport. The average measured NSF was 0.43 - in good agreement with the model predictions and the design criteria.

7.1.3 Spatial variability in sand flux within the array of straw bales

The net reduction in sand flux described above is superimposed on the spatial variability in sand flux within the straw bale array. There is considerable, but not unexpected, spatial variability within the array, as shown by Figs. 15, 16, 17, and 18, but an overall decrease downwind. The contour plots clearly indicate the higher levels of sand flux in the northwest half of the array, and also show the local variation in flux elsewhere. Some of the spatial variability is a function of sand trap location with respect to a naturally varying sand transport rate, which in turn is a result of the local topography, as well as interactions between the straw bale roughness elements and the flux of sand.

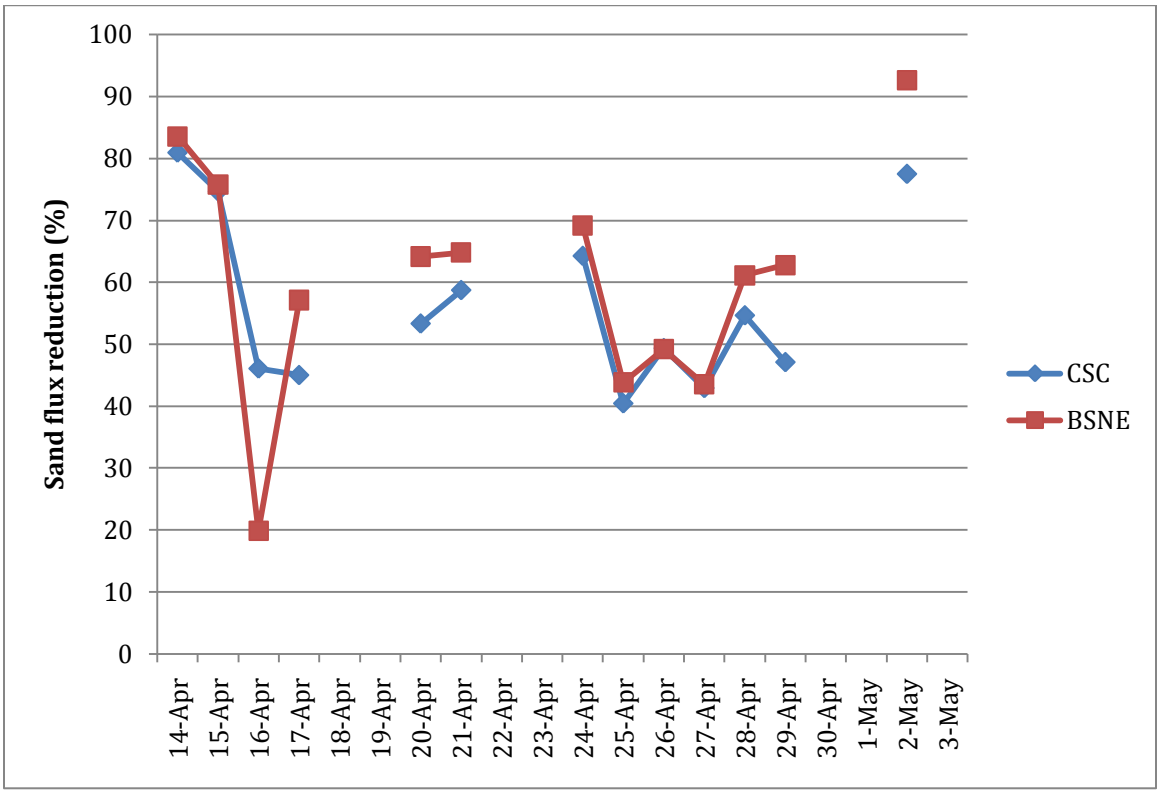

Figure 13. Time series of sand flux reduction factors (calculated using Eq.4) for the straw bale roughness demonstration plot.

Table 3. Sand flux reduction factors by trap type for the straw bale roughness demonstration plot.

	Sand flux Reduction (%)	
Date	CSC	BSNE
4/15/11	81	84
4/16/11	75	76
4/17/11	46	20
4/18/11	45	57
4/19/11	40	17
4/21/11	53	64
4/22/11	59	65
4/25/11	64	69
4/26/11	40	44
4/27/11	49	49
4/28/11	43	44
4/29/11	55	61
4/30/11	47	63
5/1/11	48	
5/3/11	78	93

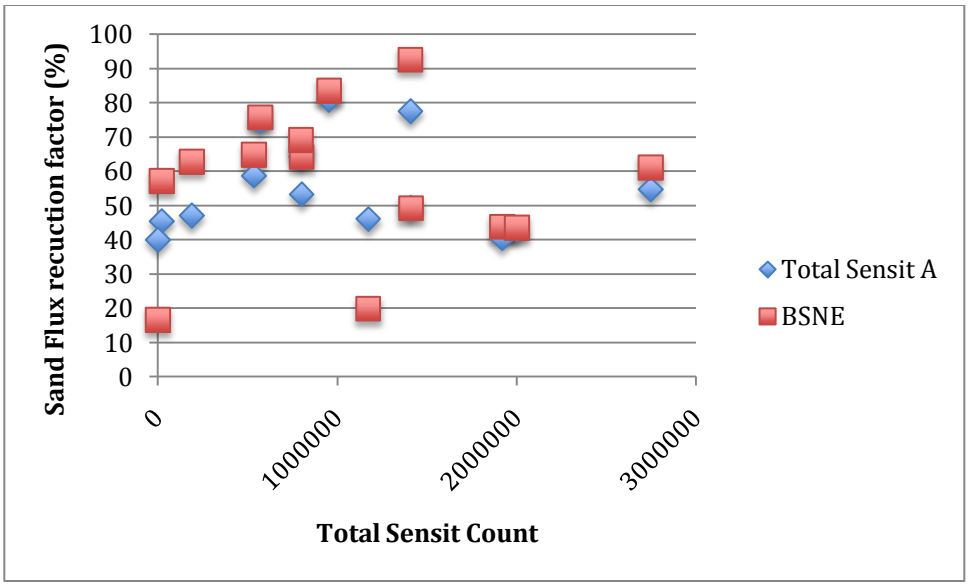

Figure 14. Relationship between sand transport event magnitude and sand flux reduction factors.

The overall picture of spatial changes in sand flux in a downwind direction is captured by the normalized sand flux (NSF), which is the sand flux at a point normalized to the upwind or incoming sand flux. Figures 19 and 20 show the change in normalized sand flux with distance downwind in the straw bale array for the different events. Note that the CSC data show a much clearer reduction in normalized sand flux compared to the single sample point represented by the BSNE traps. Figure 21 shows the average pattern of normalized sand flux over the experiment period.

All data sets indicate that sand flux is relatively higher in the first 20 m of the straw bale array and then decreases rapidly to an average of only 20% of the upwind value at 60 m into the array, and increases slightly thereafter. The higher sand flux in the western part of the area is likely the result of acceleration of flow over the low ridge that occurs within the first 40 m of the area, and is especially pronounced in the northern part of the array.

7.1.3 Durability of the straw bale array

If addition of roughness to the surface in the form of straw bales is to be adopted as a possible sand flux reduction measure on an operational scale, it is important to document its sustainability based on the pilot project installation.

Although the changes in the array of straw bales (e.g., sand erosion, deposition, burial or other deterioration of the straw bales) was not monitored in a systematic fashion during the lifetime of the pilot project, observations and repeat photographs provide some indication of the changes that occurred over the period April 15 – May 15, 2011.

Immediately (within 24 hr) of the installation of the straw bales, many of the bales experienced scour around the front (windward) side and edges, as horseshoe vortices developed around the bluff bodies of the bales. Such scour patterns have been observed in nature and wind tunnel experiments and are quite well documented (e.g., *Greeley and Iversen*, 1985; *Hesp*, 1981). The scour caused the majority of bales to tilt into the wind. Despite many sand transport events, the bales appeared to remain stable in this position for the next several weeks (Fig. 22).

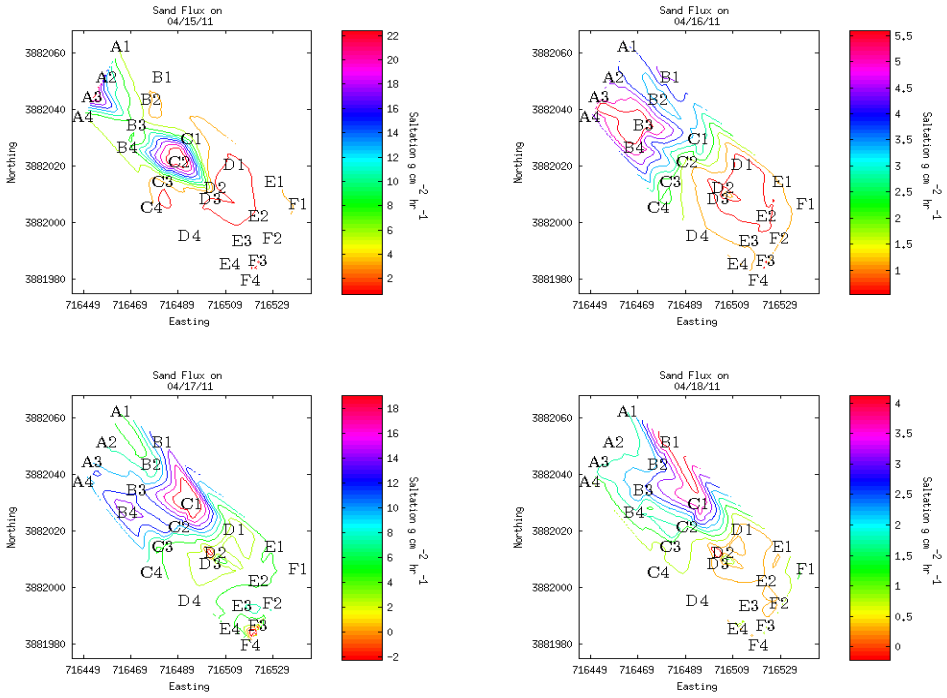

Figure 15. Spatial variation in sand flux on April 15 – April 18, 2011.

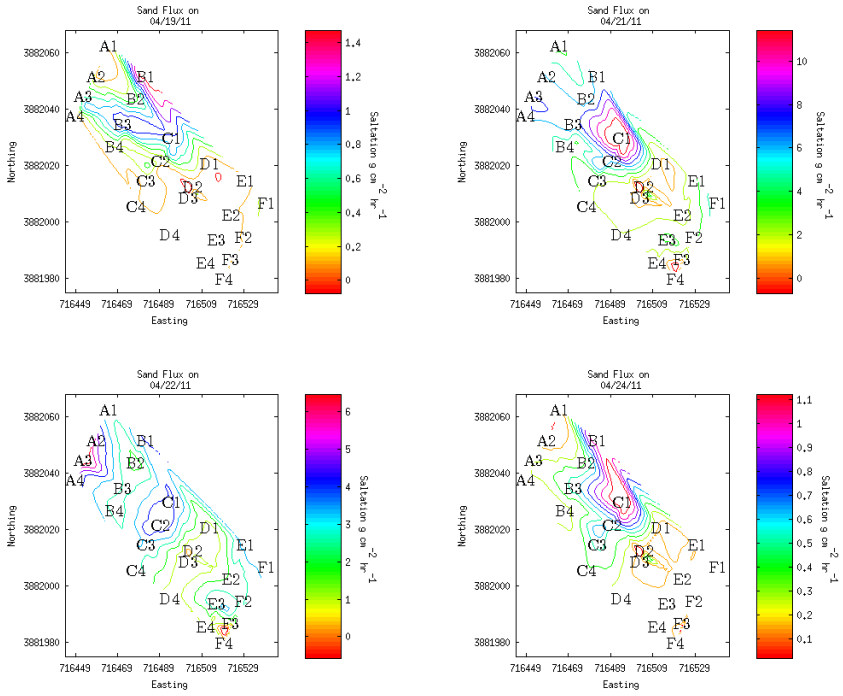

Figure 16. Spatial variation in sand flux from April 19 to April 24, 2011.

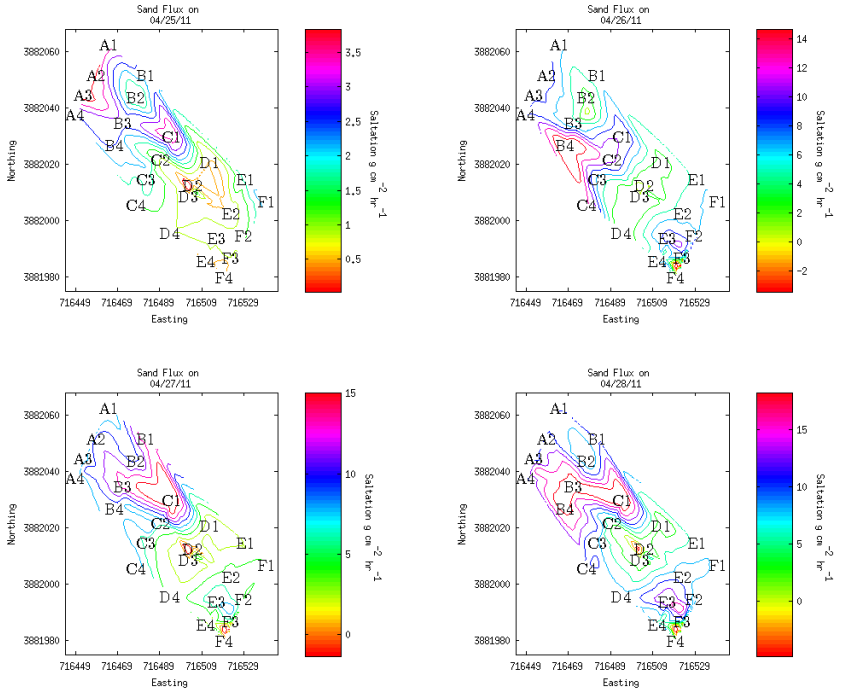

Figure 17. Spatial variation in sand flux on April 25 – April 28 2011.

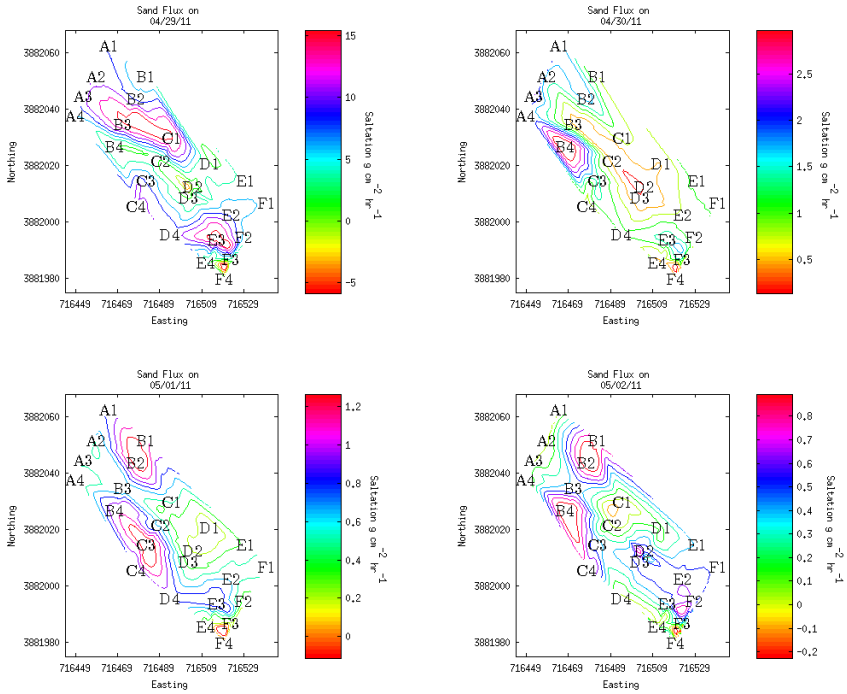

Figure 18. Spatial variation in sand flux on April 29 – May 2 2011.

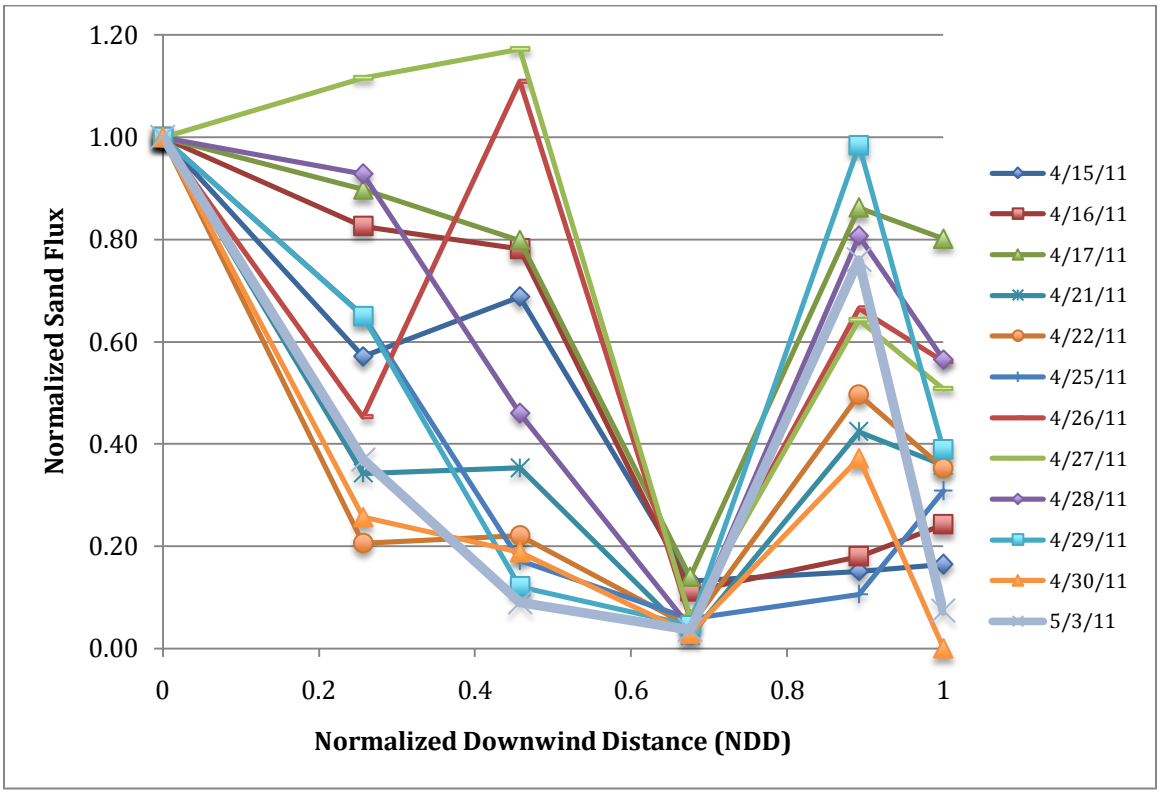

Figure 19. Variation of Normalized Sand Flux (BSNE traps) with normalized downwind distance, which is distance from the leading edge to the instrument location divided by the total distance to the furthest downwind measurement location.

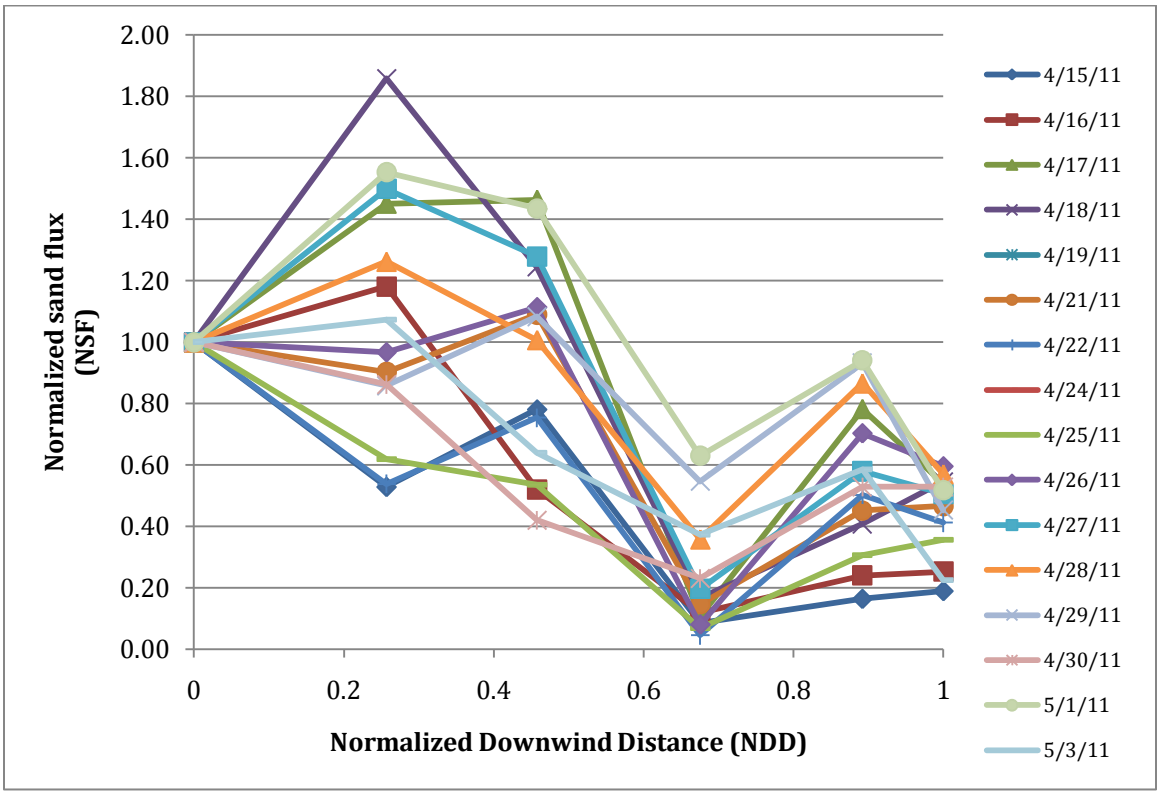

Figure 20. Variation of Normalized Sand Flux (Cox Sand Catchers) with normalized downwind distance.

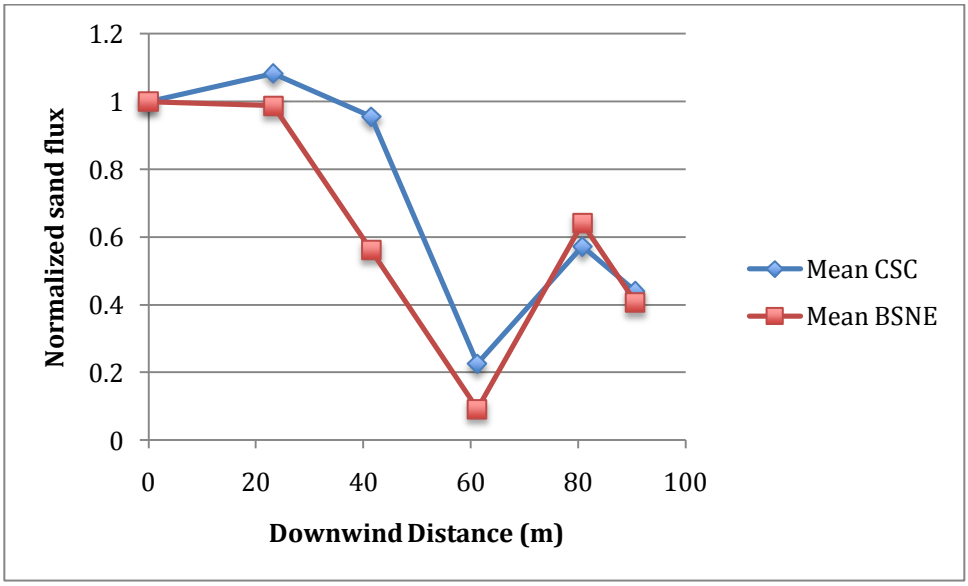

Figure 21. Variation of mean normalized sand flux with distance downwind at Straw Bale site.

Figure 22. Scour and tilting of the straw bales following installation.

During the course of the pilot projects, significant sand deposition occurred within the straw bale array (Fig. 23). This was to be expected as a result of the reduction of sand flux with distance downwind in the array, as the requirements of conservation of sediment mass and volume require that excess sediment is deposited when sand transport rates decrease in a stream-wise direction (*Middleton and Southard*, 1984).

Figure 23. Change in the straw bale array from April 15, 2011 (top) to May 15, 2011 (lower) – view to southwest.

The majority of sand deposition in the array occurred as a result of the development of shadow dunes in the lee of the bales. The shadow dunes (Fig. 24) reached a maximum height equivalent to the height of the exposed bale and extended downwind for as much as 5 m (until the next row of bales).

In addition, by mid May 2011, some bales were partially or completely buried by more widespread sand deposition. The majority of burial occurred in two main areas: (1) the southeast corner of the array – in the vicinity of sand trap rows E and F; and (2) on the north side of the array at the crest of the ridge between sand trap rows B and C.

Despite these changes, it should be noted that the sand flux reduction as a result of the straw bale array did not decline significantly throughout the pilot project lifetime. Effectiveness of the straw bales will likely diminish with increasing burial, but this relationship was not definable with the available data. No diminishment of effectiveness was observed during the study period.

Figure 24. Formation of shadow dunes downwind of straw bales

7.2 Vegetation effectiveness demonstration site

Table 4 and Figs. 25 and 26 show the reduction in sand transport at the vegetation effectiveness demonstration site. Sand flux was reduced by as much as 90-95% within the first 50 m from the upwind boundary of the vegetated area, and 90 – 99% elsewhere, as measured by the Cox Sand Catchers and BSNE traps. Minimal amounts of sand were collected in all the traps except those at the immediate upwind margin of the vegetated area, and Sensit particle counts were similarly very low and highly irregular at the Sensit within the vegetated area (Sensit D).

In many parts of the vegetated area, essentially no sand transport was recorded during the period of measurements. Sand flux at BSNE trap D, located at the downwind end of a 20-30 m-long relatively open area, was on average only 4% of that recorded in the upwind un-vegetated area.

Unlike at the straw bale roughness demonstration plot, there is no correlation between sand transport at the upwind location and within the vegetated area (Fig. 27), as indicated by sand trap or Sensit data. Even at the upwind margin of the vegetated area, the relationship is rather weak (Fig. 28)

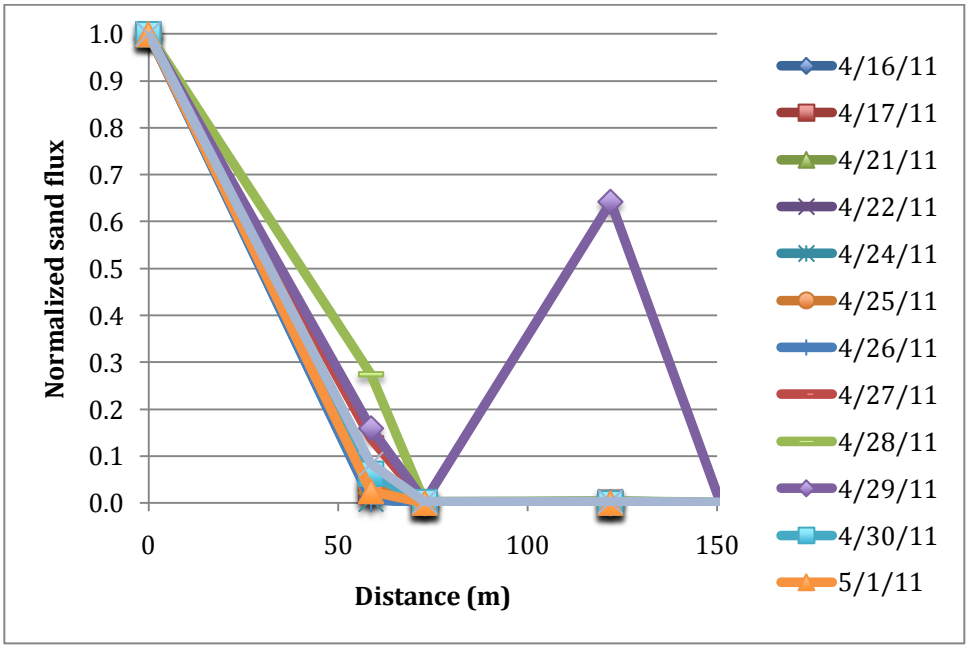

Figure 25. Variation in normalized sand flux (BSNE traps) with downwind distance at the vegetation effectiveness demonstration site.

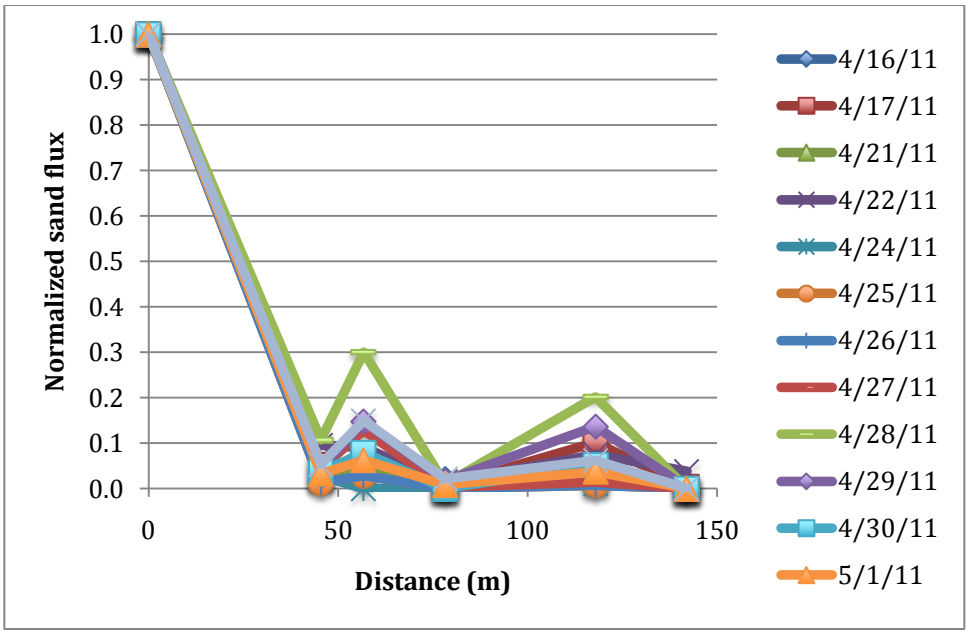

Figure 26. Variation in normalized sand flux (Cox Sand Catchers) with downwind distance at the vegetation effectiveness demonstration site.

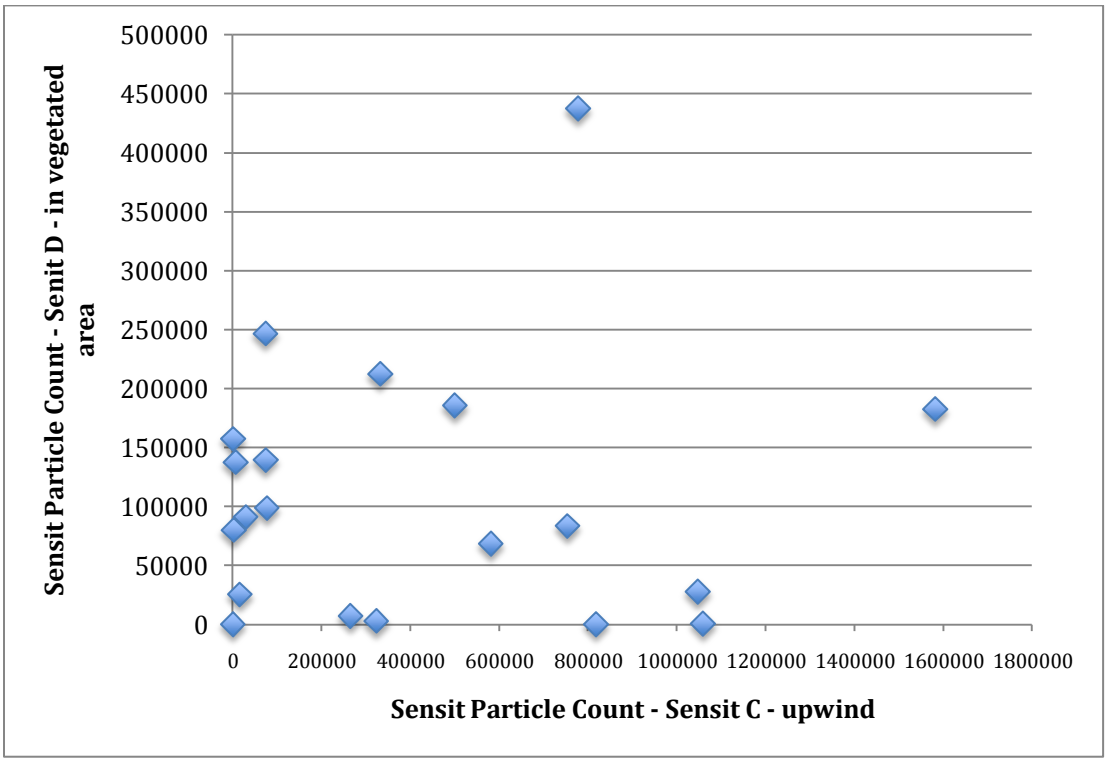

Figure 27. Relationships between sand flux and Sensit particle count upwind and within vegetated area.

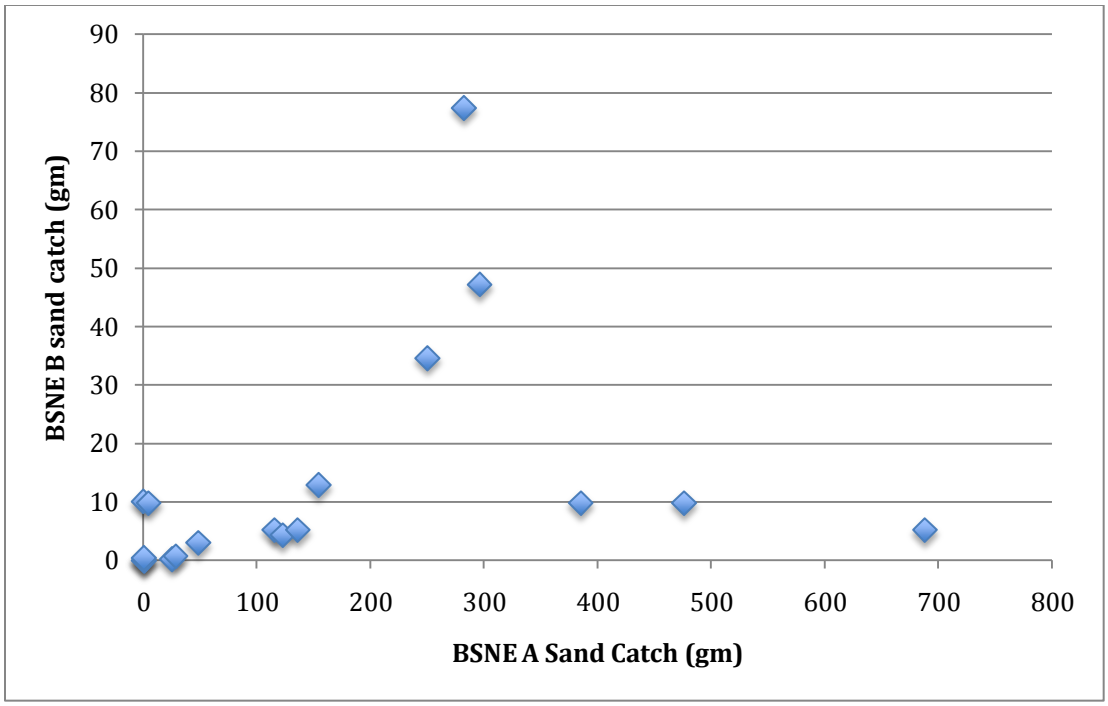

Figure 28. Relationship between sand flux upwind of vegetated area and in the immediate upwind margin of the vegetated area (BSNE B on Fig. 7).

The sand flux data from the vegetation effectiveness demonstration site clearly indicate that sand movement with the vegetated area is: (1) very low and very intermittent; and (2) that it is essentially disconnected from the transport system upwind of the area – indicating that occasional wind gusts are likely the cause of sand transport within most of the vegetated area.

Although some topographic sheltering may occur, the very low rates of sand transport within the vegetated area are primarily a direct effect of the well-established (>3 years ago), extensive, and relatively tall cover of plants (> 0.5 m), particularly lupin (*Lupinus chamissonis*). The vertically-projected cover estimated from a series of transects is 37%, with a range from 66% to 25%.; while the roughness density (λ) varies between 0.16 and 0.52. Using the graphical data in *King et al*. (2005) indicates a shear stress ratio (the ratio between the threshold [wind] shear stress required for sand transport on a bare surface and that required for a vegetated surface) of 0.1, which implies that the regional wind friction speed would need to increase by a factor of 10 to reach the threshold for transport for the sand within the vegetated area.

7.3 PM_{10} Dust Emission Potential

7.3.1 Straw bale roughness demonstration site

Results from the tests at the straw bale roughness demonstration site are shown in Fig. 29. Note that the y-axis is on a logarithmic scale for clarity. Panel *a* shows a summary of the measurements completed with the black PI-SWERL while panel *b* shows a summary of the measurements completed with the brown PI-SWERL. In both cases, PM_{10} dust emissions are plotted for varying values of equivalent smooth surface friction speed. Shear stress, as quantified by the wind friction speed, drives the sediment transport system, however this quantity can be converted to provide an estimate of wind speed at a typical reference height (e.g., 10 m) using boundary-layer theory and an estimate of the aerodynamic roughness length

(z_o) of the surface. Using data available from the SI tower a mean aerodynamic roughness length was estimated to be 0.00026 m. Wind speed at a reference height can be calculated using the relationship:

$$\frac{u_z}{u_*} = \frac{1}{\kappa} ln\left(\frac{z}{z_o}\right) \quad (6)$$

where u_z is the wind speed at height z, u_* is wind friction speed, κ is von Kármán's constant (0.4). Wind friction speed is related to shear stress (τ) by the relationship:

$$\tau = \rho u_*^2 \quad (7)$$

where ρ is air density. The equivalent wind speed at 10 m that corresponds to the PI-SWERL friction speed set points are included on all subsequent figures for reference to observable wind conditions. We note that these wind speeds are only approximate and that in fact, the 10 m equivalent wind speed for a given value of wind friction speed will vary depending on local surface roughness, which can in turn vary considerably. For the purposes of this report, an equivalent wind speed that is calculated with the aid of Eq. 6 provides an estimate that is accurate to within approximately $\pm$15%. This range is bound at the upper end by assuming that the local roughness could be five times smaller than the assumed value (0.00026 m) and at the lower end by assuming that the local roughness could be five times larger than the assumed value.

Also shown in Fig. 29 are the OGS counts from the two OGS sensors that are mounted at 15 cm above the test surface (OGS3 and OGS4). The two OGS sensors mounted near the surface (4 cm) provided highly erratic results owing to the extremely high levels of sand movement there. Note that even the two sensors that are mounted away from the surface registered values near where the sensors would be considered saturated (especially for friction velocities of 0.55 m/s or greater). The OGS sensors that are mounted further away from the test surface cannot provide an accurate estimate of sand movement that can be related to an independently measured sand flux (e.g., by sand trap). However, they do provide an indication of the magnitude of sand movement. That is, the greater the OGS counts (up to the saturation limit), the greater the sand movement.

There are some clear trends that can be discerned from Fig. 29. First, it is very clear that PM_{10} dust emissions increase with increasing wind friction speed. Second, sand movement as quantified by the two OGS sensors within the PI-SWERL that were not consistently saturated (with the previously mentioned caveat that the sensors exhibit saturation behavior for wind friction speed of 0.55 m/s or greater) also increases with friction speed. In fact, sand movement and dust emissions are highly correlated ($r > 0.9$ in all cases), reinforcing the basic underlying assumption that dust emissions at the Oceano Dunes are driven by sand movement. Third, although there appear to be some differences in PM_{10} dust emissions at the lower values of wind friction speed examined, overall, the measurements from the black and brown PI-SWERLs were quite similar (panel c of Fig. 29). This is reassuring since the two PI-SWERLs were conducting measurements on essentially the same surface at the same moment in time.

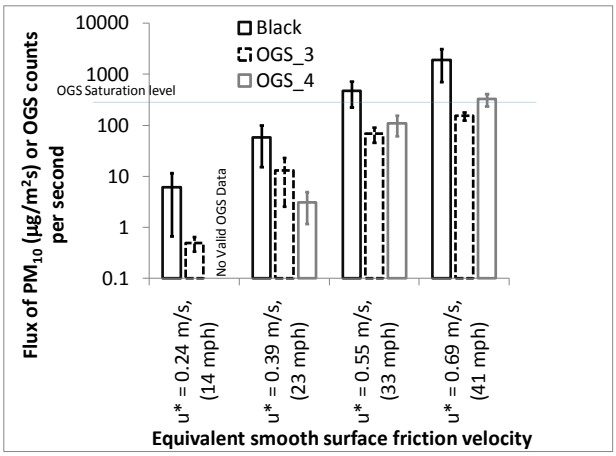

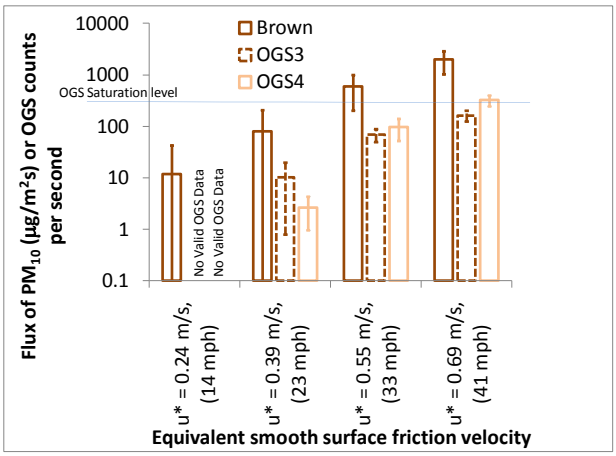

a. PM_{10} dust emissions and OGS - black b. PM_{10} dust emissions and OGS - brown

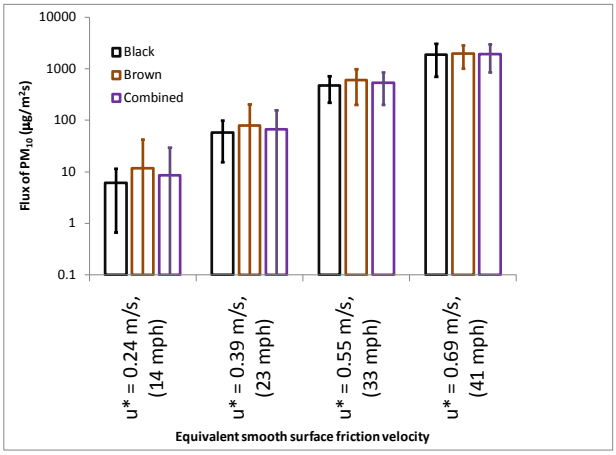

c. PM_{10} dust emissions from black and brown PI-SWERL and combined emissions. Error bars represent standard deviations.

Figure 29. Results from PI-SWERL tests at the straw bale roughness demonstration site. Equivalent wind speeds calculated assuming roughness height z_0 is approximately 0.00026 meters.

The threshold wind speed at which sediment transport begins is an important aspect for understanding the dust emission system. Defining that threshold for dust emissions is not straightforward. According to Shao (2000), the stochastic nature of particle entrainment is its defining feature. Shao (2000) suggests that for dust entrainment it would be desirable to characterize u_{*t} as a distribution including the statistical parameters of mean, median, and standard deviation. For the Oceano Pilot studies defining threshold would require a set of rules be adopted to apply to the PM_{10} emission data gathered with the PI-SWERL, specifically during the initial ramp phase from 0 to 1000 rpm. At this time developing an estimate of threshold wind speed from these data is not viewed as a critical component needed to evaluate the effectiveness of the pilot projects. In lieu of a PI-SWERL derived threshold the wind speed and saltation activity data from the S1tower are used to provide an estimate on the regional wind speed measured at 10 m required to initiate sand transport, and the associated dust emissions in the study domain. Using the z_o value derived for the S1 tower and the saltation activity data from there, sand transport in the absence of roughness (bales or vegetation) was estimated to initiate at a wind speed of 5.3 m/s (12 mph), which corresponds to a friction speed of 0.20 m/s. Note that data from the PI-SWERL OGS sensors provide inferential support for this estimate of threshold friction speed as evidenced by some sand movement activity at a friction velocity of 0.24 m/s.

7.3.2 Vegetation effectiveness demonstration site

The results from the vegetation-stabilized site point to very similar trends (Fig. 30) and will be discussed later in the context of comparing the magnitudes of emissions from the three different locations where PI-SWERL measurements were conducted.

7.3.3 ATV – exclosure transect site

Figure 31 shows the measurement results from the tests along the exclosure fence. An important question to address is whether or not there is a significant difference in PM_{10} dust emissions between the sand inside the exclosure and the sand outside the exclosure (traveled on by recreational vehicles). It appears that dust emissions measured outside the exclosure (black PI-SWERL) are systematically higher than those within the exclosure. An unpaired single-sided t-test assuming unequal variances yields P-values of 0.090, 0.005, 0.006, and 0.003 for comparisons at friction speeds of 0.24 m/s (14 mph), 0.39 m/s (23 mph), 0.55 m/s (33 mph), and 0.69 m/s (41 mph), respectively. The values in the brackets are the wind speeds at 10 m above the ground given in miles per hour to facilitate comparison with standard meteorological measurements. Statistically, this indicates that the dust emissions measured by the black PI-SWERL (outside exclosure) were higher for the three highest friction speeds tested as compared to the emissions measured by the brown PI-SWERL (inside exclosure) at the 0.05 significance level.

As mentioned previously, the DustTrak that was used primarily with the PI-SWERL outside the exclosure was exhibiting spuriously high concentrations. The concentrations were corrected subsequently following laboratory collocation with the DustTrak used inside the exclosure. However, the reason for the DustTrak's behavior was not uncovered and there remains some uncertainty about whether the correction factor applied was without bias. With this caveat, measured dust emissions outside of the exclosure were higher than inside by 56%, 49%, 70%, and 70% at the four set equivalent wind friction speeds.

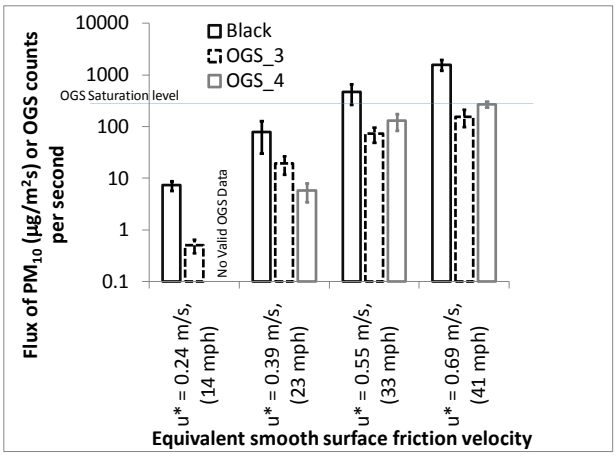

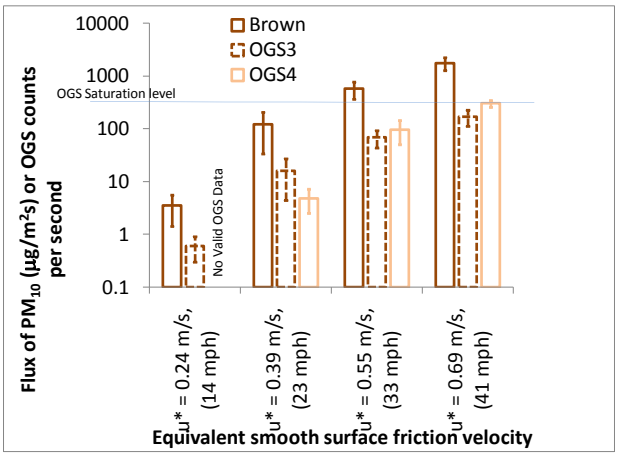

a. PM_{10} dust emissions and OGS - black b. PM_{10} dust emissions and OGS - brown

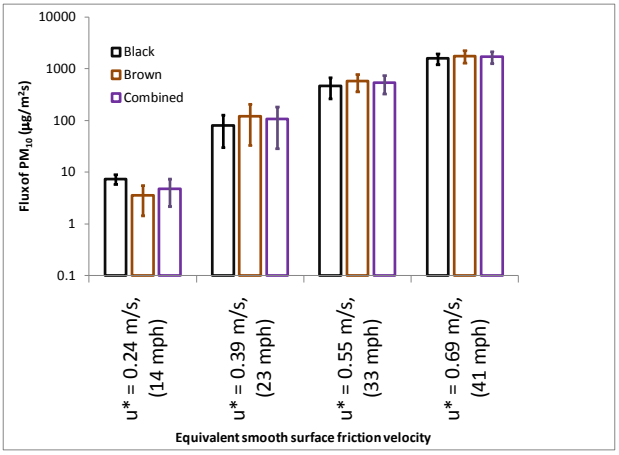

c. PM_{10} dust emissions from black and brown PI-SWERL and combined emissions. Error bars represent standard deviations.

Figure 30. Results from PI-SWERL tests at the vegetation demonstration site. Equivalent wind speeds calculated assuming roughness height z_0 is approximately 0.00026 meters.

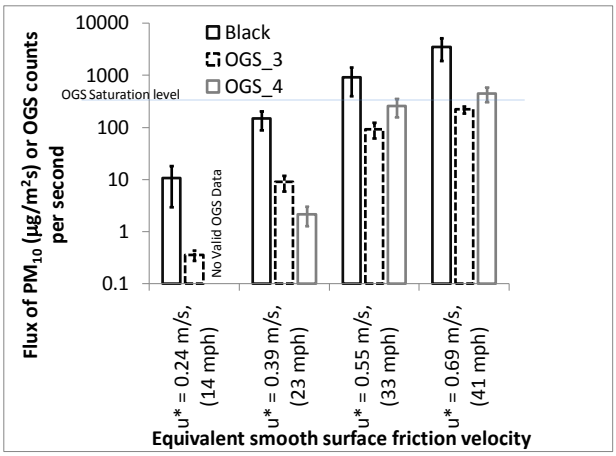

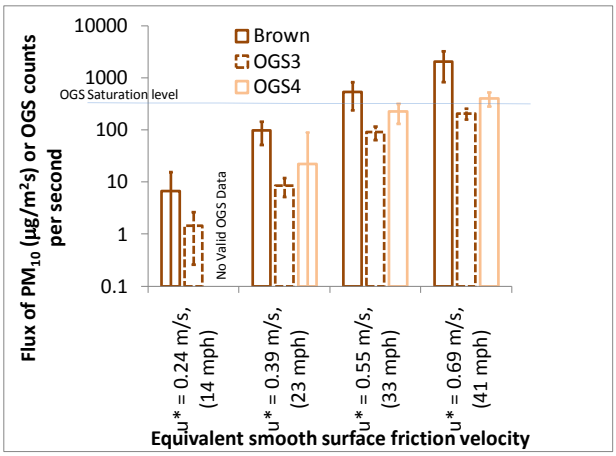

a. PM_{10} dust emissions and OGS - black b. PM_{10} dust emissions and OGS - brown

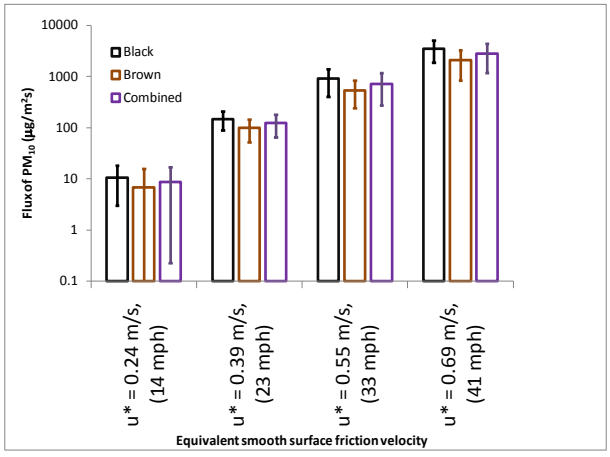

c. PM_{10} dust emissions from black and brown PI-SWERL and combined emissions. Error bars represent standard deviations.

Figure 31. Results from measurements along exclosure fence (black was outside exclosure, brown was within exclosure). Equivalent wind speeds calculated assuming roughness height z_0 is approximately 0.00026 meters.

The combined measurements of the two PI-SWERLs are compared for the three different locations in Fig. 32 and tabulated in Table 5. There appear to be some minor differences in dust emissions among the three different sites. Comparing dust emissions measured with the Brown PI-SWERL only, there are no statistically significant differences among emissions at the straw bale site, vegetated dune site, and the exclosure area (Table 5). Similarly, there are no significant differences between emissions measured with the black PI-SWERL at the straw bale site and the vegetated site. Measurements using the black PI-SWERL outside of the exclosure site were statistically different than those obtained at either the vegetated or straw bale site. However, some of the same caveats applied to the comparison of emissions measured inside and outside the exclosure also apply here (i.e., unexplained drift in DustTrak calibration on 4/14/11). Panel b of Fig. 32 shows power law fits to the emissions as a function of equivalent friction speed. These empirical fits can be used to estimate the reductions in dust emissions that can be gained through shear-stress partitioning-type control approaches.

7.4 Particle Size Analysis

The average particle size distributions of the sand-sized component of the selected samples as a function of pilot test location expressed as percent weight are shown in Fig. 33. The average percent and standard deviation of the average sand (2000 – 63 μm, silt (63 – 2 μm), and clay (<2 μm) fractions for the samples from each pilot test area are shown in Table 4.

Table 4. Textural characteristics of the pilot test sites.

Site	Average % Sand	Std. Dev. % Sand	Average % Silt	Std. Dev. % Silt	Average % Clay	Std. Dev. % Clay
Straw Bales	99.52	0.15	0.25	0.07	0.28	0.04
Vegetation	99.24	0.51	0.54	0.37	0.16	0.04
ATV	99.57	0.13	0.20	0.06	0.20	0.06
Exclosure	99.37	0.18	0.31	0.12	0.24	0.07

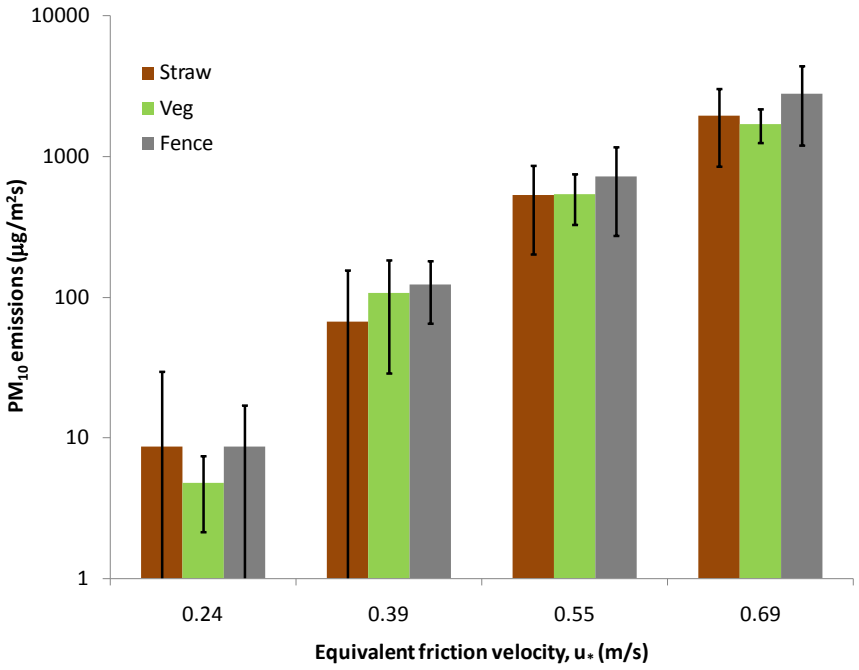

a. Comparison of PM_{10} dust emissions magnitudes across three locations

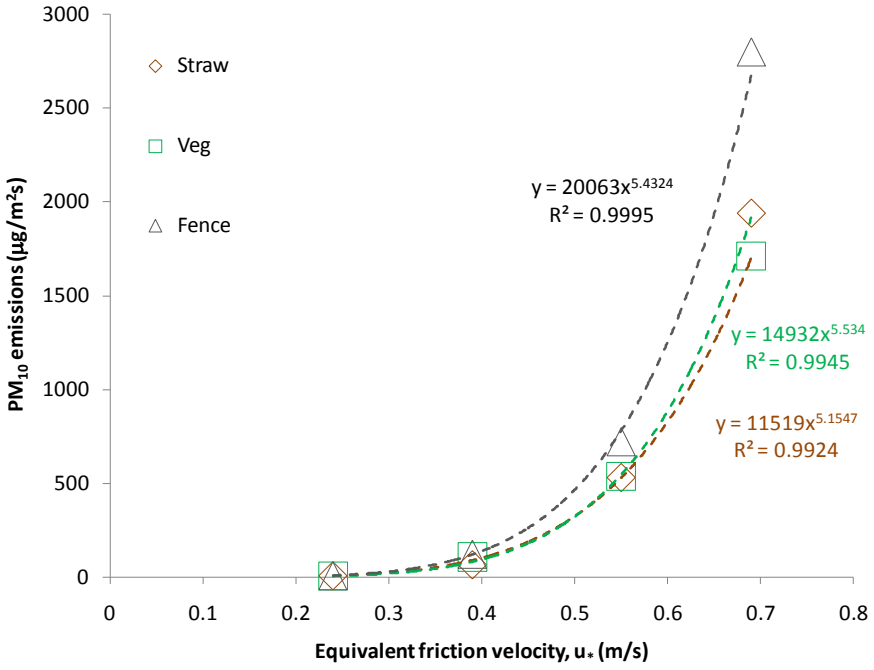

b. Power fits to PM_{10} dust emissions for measurements at three locations

Figure 32. Relative magnitudes of emissions from straw bale, vegetated, and along-fence measurements using combined data from both PI-SWERLs. Equivalent wind speeds calculated assuming roughness height z_0 is approximately 0.00026 meters with a possible range of 0.000052 to 0.0013 meters.

Table 5. One and two-sided t-test results for samples of unequal variances. Highlighted cells indicate a statistically significant finding at the α = 0.05 level.

Hypothesis	u* (m/s)/(approx. 10-m wind speed in mph)	0.24 / (14)	0.39 / (23)	0.55 / (33)	0.69 / (41)
Location 1: Straw bale site	Mean 1 / Mean 2 (ug/m2s)	6 / 12	57 / 79	476 / 602	1907 / 1979
Location 2: Straw Bale Site	Var 1 / Var 2 (ug/m2s)	30 / 995	1765 / 16379	64629 / 161132	1450629/902772
PI-SWERL 1 (Black) different	# tests 1 / # tests 2	19 / 15	19 / 15	19 / 15	19 / 15
from PI-SWERL 2 (Brown)?	P- value (one sided) / P-Value (two sided)	0.253 / 0.506	0.267 / 0.535	0.151 / 0.301	0.424 / 0.847
Location 1: Vegetated site	Mean 1 / Mean 2 (ug/m2s)	7 / 4	79 / 121	466 / 574	1579 / 1777
Location 2: Vegetated site	Var 1 / Var 2 (ug/m2s)	2 / 4	2410 / 7627	41289 / 44868	140543/243219
PI-SWERL 1 (Black) different	# samples 1 / # samples 2	7 / 14	7 / 14	7 / 14	7 / 14
from PI-SWERL 2 (Brown)?	P- value (one sided) / P-Value (two sided)	0.000 / 0.000	0.091 / 0.181	0.139 / 0.278	0.161 / 0.321
Location 1: Fence ATV	Mean 1 / Mean 2 (ug/m2s)	11 / 7	148 / 99	910 / 536	3531 / 2073
Location 2: Fence Exclosure	Var 1 / Var 2 (ug/m2s)	57 / 81	3538 / 2253	254968/87632	2671215/1518479
PI-SWERL 1 (Black) different	# samples 1 / # samples 2	18 / 18	18 / 18	18 / 18	18 / 18
from PI-SWERL 2 (Brown)?	P- value (one sided) / P-Value (two sided)	0.090 / 0.179	0.005 / 0.011	0.006 / 0.011	0.002 / 0.005
Location 1: Straw bale site	Mean 1 / Mean 2 (ug/m2s)	12 / 4	79 / 121	602 / 574	1979 / 1777
Location 2: Vegetated site	Var 1 / Var 2 (ug/m2s)	995 / 4	16379 / 7627	161132/44868	902772/243219
PI-SWERL 1 (Brown) different	# samples 1 / # samples 2	15 / 14	15 / 14	15 / 14	15 / 14
from PI-SWERL 2 (Brown)?	P- value (one sided) / P-Value (two sided)	0.166 / 0.331	0.158 / 0.315	0.408 / 0.817	0.239 / 0.477
Location 1: Vegetated site	Mean 1 / Mean 2 (ug/m2s)	4 / 7	121 / 99	574 / 536	1777 / 2073
Location 2: Fence exclosure	Var 1 / Var 2 (ug/m2s)	4 / 81	7627 / 2253	44868/87632	243219/1518479
PI-SWERL 1 (Brown) different	# samples 1 / # samples 2	14 / 18	14 / 18	14 / 18	14 / 18
from PI-SWERL 2 (Brown)?	P- value (one sided) / P-Value (two sided)	0.080 / 0.160	0.209 / 0.418	0.339 / 0.678	0.182 / 0.364
Location 1: Straw bale site	Mean 1 / Mean 2 (ug/m2s)	12 / 7	79 / 99	602 / 536	1979 / 2073
Location 2: Fence exclosure	Var 1 / Var 2 (ug/m2s)	995 / 81	16379 / 2253	161132/87632	902772/1518479
PI-SWERL 1 (Brown) different	# samples 1 / # samples 2	15 / 18	15 / 18	15 / 18	15 / 18
from PI-SWERL 2 (Brown)?	P- value (one sided) / P-Value (two sided)	0.280 / 0.560	0.286 / 0.573	0.303 / 0.605	0.403 / 0.806
Location 1: Straw bale site	Mean 1 / Mean 2 (ug/m2s)	6 / 7	57 / 79	476 / 466	1907 / 1579
Location 2: Vegetated site	Var 1 / Var 2 (ug/m2s)	30 / 2	1765 / 2410	64629/41289	1450629/140543
PI-SWERL 1 (Black) different	# samples 1 / # samples 2	19 / 7	19 / 7	19 / 7	19 / 7
from PI-SWERL 2 (Black)?	P- value (one sided) / P-Value (two sided)	0.191 / 0.383	0.161 / 0.322	0.459 / 0.919	0.151 / 0.301
Location 1: Vegetated site	Mean 1 / Mean 2 (ug/m2s)	7 / 11	79 / 148	466 / 910	1579 / 3531
Location 2: Fence ATV	Var 1 / Var 2 (ug/m2s)	2 / 57	2410 / 3538	41289/254968	140543/2671215
PI-SWERL 1 (Black) different	# samples 1 / # samples 2	7 / 18	7 / 18	7 / 18	7 / 18
from PI-SWERL 2 (Black)?	P- value (one sided) / P-Value (two sided)	0.054 / 0.107	0.006 / 0.011	0.002 / 0.005	0.000 / 0.000
Location 1: Straw bale site	Mean 1 / Mean 2 (ug/m2s)	6 / 11	79 / 148	476 / 910	1907 / 3531
Location 2: Fence ATV	Var 1 / Var 2 (ug/m2s)	30 / 57	16379 / 3538	64629/254968	1450629/2671215
PI-SWERL 1 (Black) different	# samples 1 / # samples 2	19 / 18	15 / 18	19 / 18	19 / 18
from PI-SWERL 2 (Black)?	P- value (one sided) / P-Value (two sided)	0.026 / 0.052	0.035 / 0.070	0.002 / 0.003	0.001 / 0.002

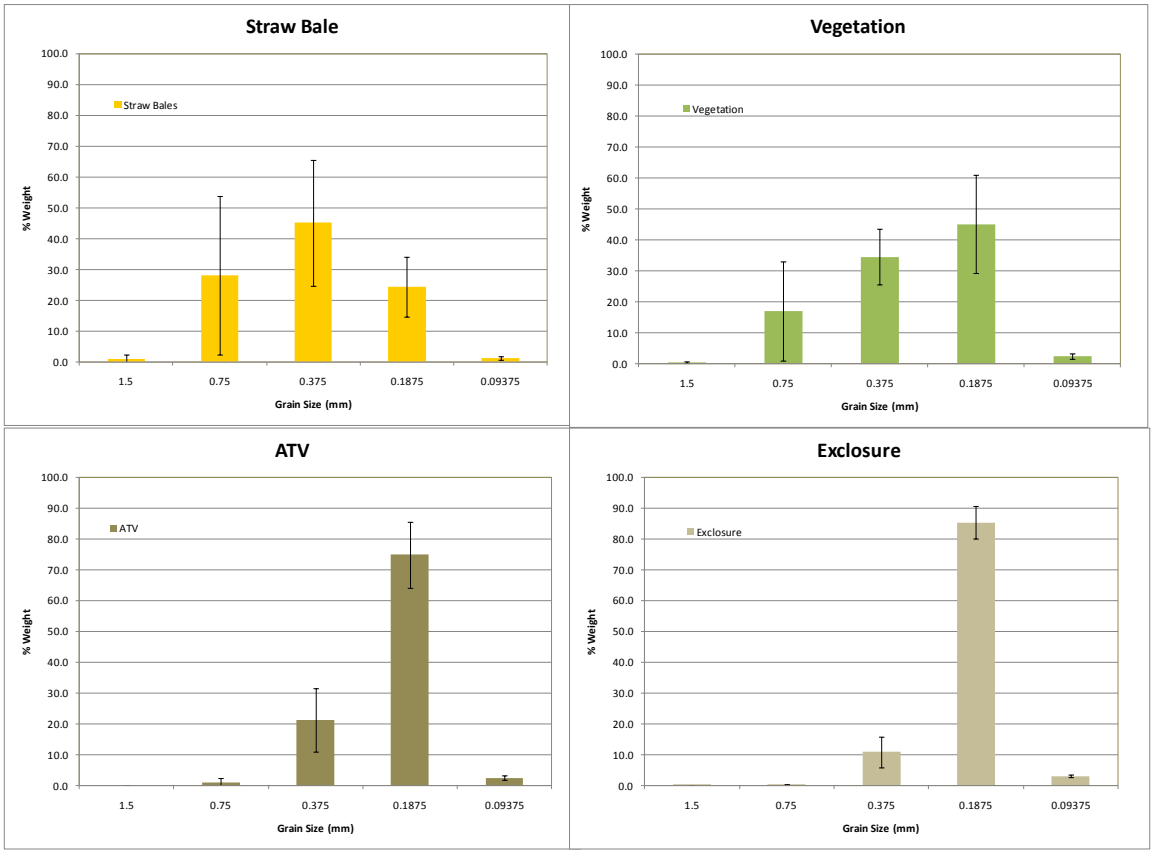

Figure 33. Average particle size distributions of the sand-sized fraction for each of the pilot project test area. These represent average values from the multiple samples submitted from each location with the error bars representing the standard deviation of the mean.

The particle size data indicate, as expected, an environment dominated by the sand fraction. For all three pilot test sites the total sand content is greater than 99%. Between sites there is some variation in the mean sand diameter from a low of 171 µm (±15.9 µm) for the exclosure area to 315.6 µm (±100.8 µm) for the straw bale site. The energy imparted to the surface upon impact of particles of these sizes, for equivalent particle speed, is ≈1.8 times greater for the larger diameter particle (Dong et al., 2002), which would have only a small effect on dust emissions. The available texture data for the three size classes sand, silt, and clay, show a consistent distribution of the percent silt and clay fractions varying in the silt fraction from 0.54% (±0.37%) for the vegetation site to 0.25% (±0.07%) for the straw bales and for the clay fraction 0.28% (±0.04%) for the straw bale site to 0.16% (±0.04%) for the vegetation site. These data support the PI-SWERL data that shows the variability in PM_{10} emissions among the test sites to be modest, generally less than a factor of 1.75 between the most emissive area (near fence locations) and the least emissive straw bale site (Fig. 32b). This follows from the result that the amount of silt and clay in the dune sands within the pilot projects sites is very similar regardless of location on the dunes.

8. Discussion

8.1. Straw bale roughness demonstration site

The straw bale roughness demonstration site results provide corroborative evidence that the relation between roughness density and sand flux reduction as defined by *Gillies et al*. (2006) is suitable for planning a sand flux reduction strategy using solid elements that approximate the size of straw bales (Fig. 34). Importantly the data obtained from the roughness demonstration site also indicates that the predictive relationship applies for the conditions of essentially no transport limitations, i.e., the strength of the wind controls, for the most part, the amount of sand moved. The measurements of sand transport reduction in *Gillies et al*. (2006) were made under the condition of supply limitation. The corroboration of the relationship presented by *Gillies et al*. (2006) with the new data from Oceano also supports their earlier finding that larger roughness elements are more efficient in reducing sand transport than smaller elements for equivalent roughness densities. If small elements (height ≈ 0.10 m) like those studied by *Lancaster and Baas* (1998) had been used no measureable effect of roughness on sand transport would have been observed for the condition of $\lambda = 0.020$. To achieve similar control for 0.1 m high elements would have required a roughness density of 0.055 and the positioning of 55,000 individual 0.1 m high × 0.1 m long × 0.1 m wide elements.

Demonstrating that element size is a critical feature of roughness in controlling sand flux under conditions of essentially limitless sediment supply is very important as much higher levels of control can be achieved with lower numbers of large roughness elements, such as readily available straw bales. Using large elements is more logistically feasible and likely more economical and more effective than having to deploy larger numbers of small elements.

An estimation of the reduction in PM_{10} emissions resulting from the positioning of the straw bales can be estimated through the application of the *Raupach et al*. (1993) shear stress partitioning equation and the PM_{10} emission relationship for the surface as measured by the PI-SWERL prior to placing the bales on the surface. Using the mean grain size for the sand at this pilot site of 316 μm, the predicted threshold wind friction speed is approximately 0.2 m/s based on the relationship of *Bagnold* (1941), in the absence of any roughness, which is the same value as estimated for the S1 tower (see Section 7.3.1). Following the addition of the straw bales the *Raupach et al*. (1993) model, based on the known or assumed values for the input parameters (i.e., σ=0.786, λ=0.0201, β=231.9, and m=0.7 [m is from *Gillies et al*., 2006]) the regional friction speed required to cause the sand to move within the array of straw bales would need to reach 0.30 m/s, which corresponds to a wind speed of 7.9 m/s (17.7 mph) measured at 10 m above the surface. The increase in the regional friction speed to cause transport could reduce the overall PM_{10} burden as there may be fewer transport events due to the necessity of higher winds to activate the sediment transport and dust emissions system.

Using the PM_{10} emission relationship shown in Fig. 32 for the straw bale test surface and the shear stress partitioning effect as predicted by *Raupach et al*. (1993), which estimates that 48% of the regional shear stress reaches the intervening surface among the straw bales, would result in a lowering of the PM_{10} emissions as a function of wind friction speed by ≈98% (for all friction speeds above the sand transport threshold), as compared with the surface in the absence of straw bale roughness. This is due to the non-linear relationship between dust emissions and friction speed as demonstrated for the PI-SWERL derived dust emission relationship shown in Fig. 32b. For example, if the regional friction speed as measured above the straw bales was 0.55

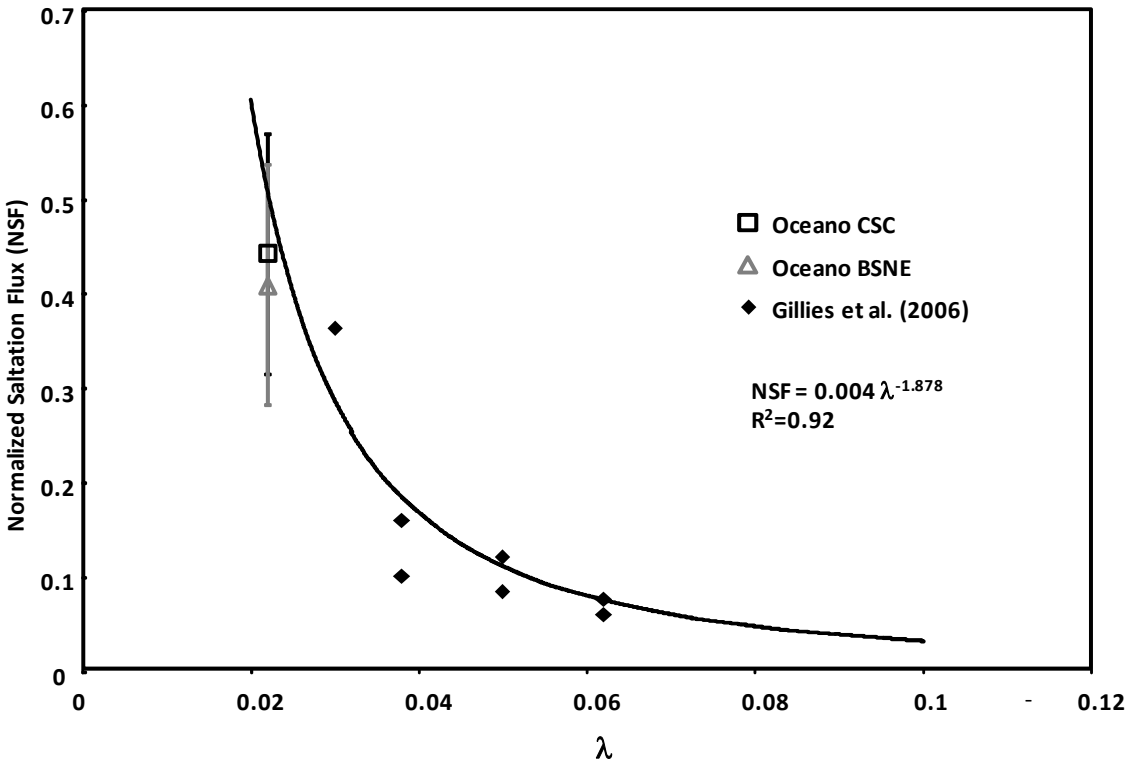

Figure 34. Normalized mean saltation flux (NSF) as a function of λ including data from both trap types at Oceano and the data from Gillies et al. (2006). The regression-derived relationship is for all data combined. Error bars on the Oceano data points represent the standard deviation of the mean.

m/s, the friction speed acting on the intervening surface among the straw bales would be 0.26 m/s so the predicted PM_{10} emissions originating from the straw bale site would be ≈12 μg/m^2 s as opposed to ≈529 μg/m^2 s in the absence of that roughness using the relationship for the straw bale site as presented in Fig. 32b.

Unfortunately due to the unforeseen problem of the OGS sensors in the PI-SWERL exceeding their measurement capability when the counts exceeded 250 per second we cannot at this time present PM_{10} emission measurements as a function of sand transport as originally anticipated.

Manipulating the surface roughness to reduce PM_{10} emissions and/or to influence sand deposition patterns holds good promise as a control strategy for the Oceano Dunes. The sand transport and roughness data collected as part of this project clearly corroborates the published relationship of *Gillies et al*. (2006) linking sand transport reduction to roughness density, which provides quite high confidence that it can be used to aid in the design of surface roughness configurations to modify sand transport and the associated dust emissions.

8.2 Vegetation demonstration site

The PI-SWERL PM_{10} emission data (Fig. 30 and 32b) indicate that the sand in which the plants are situated has the potential to emit PM_{10} at levels similar to the other Pilot study locations,

but the probability of emissions occuring is low. The vegetation demonstration site sand reduction data clearly indicate the effectiveness of this amount and size of vegetation cover to dramatically reduce sand transport and the associated emission of PM_{10}, due to the reduction in surface wind shear afforded by the plants. In the three years of growth following the planting of the vegetation the level of control on sand movement and dust emissions is almost 100%. Clearly this control method where applicable can offer a very effective solution

8.3 ATV and vehicle exclosure demonstration site

Restricting vehicle access to dune areas has been proposed as a means to reduce PM_{10} emissions, and hence lower the regional PM_{10} concentrations downwind of the dunes. The PI-SWERL data suggest that the PM_{10} emission potential is reduced within the exclosure area as compared to the area with off-road driving allowed for equivalent wind friction speeds. As stated in the results sections for the u_* values: 0.24, 0.39, 0.55, and 0.69 m/s were 56, 49, 70, and 70% higher in the driving-allowed area where measurements were taken versus inside the exclosure area where driving was not permitted. As mentioned in the results section there was some difficulty with one of the DustTrak devices used in one of the PI-SWERLs in the field and we developed a relationship to adjust the data collected with that instrument post-field work (Fig. 10). Based on the areal extent of the Oceano Dunes driving-allowed and driving-restricted areas, the pilot study measurements represent a very small area that may not be representative of the environments as a whole. The PM_{10} emission data from the other pilot locations does, however, suggest that variability in PM_{10} emissions between sites that are kilometers apart was not high (Table 5) so that variability between the exclosure are and the driving area could be expected to be limited as well. The observations of limited variability in PM_{10} emission potential across the pilot test sites is corroborated by the texture measurements (Table 4), which also show very limited differences in the silt and clay components of the sediments, wherein the PM_{10} particles for the most part reside.

8.4 Particle Size Distributions

The particle size data indicate that the pilot project test areas are dominated by the sand fraction, with some variation in the mean diameter of this fraction. Texturally the collected samples from all locations are essentially identical with the silt and clay size fraction combined accounting for approximately 0.5%. However, in terms of available particles as a source of PM_{10}, it is obviously not inconsequential. In 1 m^3 of Oceano Dune sand (assuming a bulk density of 1602 kg/m^3, a typical industry standard for quartz sand [source: http://www.simetric.co.uk/si_materials.htm]) there would be approximately 3.5 kg of clay-sized particles (physical diameter <2 μm). This 1 m^3 of sand holds enough material to create 2.3×10^7 m^3 of air that would have a mass concentration of dust of 150 $\mu g/m^3$, which is the Federal 24-hour PM_{10} air quality standard, if all the dust-sized material was released into the air during saltation.

9.0 Conclusions

This pilot study was designed to evaluate the effectiveness of three control strategies to reduce PM_{10} emissions from the Ocean Dunes. Two of the control strategies were based on modifying the sand surface by increasing the surface roughness through the addition of large roughness elements. In one case the surface was modified through placement of solid, rectangular elements (straw bales), and in the second case planted vegetation acted as the surface modifier.

For both cases a high degree of sand movement control was observed, and by extension dust emissions were significantly reduced. The control of emissions by roughness is principally by the need for higher winds to cause emissions to occur, which reduces the range of wind speeds over which emissions will occur, and by partitioning of the available shear stress between the roughness elements and the surface. At equivalent regional friction speeds the straw bale roughness allows only 48% of the shear stress to reach the surface, thus reducing PM_{10} production potentially by 98%, based on the PI-SWERL derived PM_{10} emission relationship (Fig. 32b). The vegetation pilot site has even great PM_{10} reduction due to the presence of the more extensive coverage by the plants. The roughness control method as tested in two configurations is a highly effective for PM_{10} control and could form the basis for viable control strategies at Oceano Dunes. The effectiveness of the roughness to reduce PM_{10} emissions is related directly to the decrease in wind shear and sand flux in these environments as compared to sand flux in the absence of roughness (bales or vegetation).

An example of using roughness to modifying the Oceano Dune surface and thus moderate PM_{10} emissions would be to use solid element roughness such as straw bales to initiate the development of a fore-dune system at an appropriate distance from the high water line. Sand would build up in the roughness, thus removing it from further transport and the associated PM emissions that would be associated with the saltation process. Vegetation could be planted in the roughness array in protected areas with the objective being that the vegetation would eventually become self-sustaining and become the dominant roughness control such that the straw bale roughness could be allowed to decay.

The effectiveness of restricted driving to reduce PM_{10} emissions is less certain than the clear results from the roughness demonstration projects. The PM_{10} emission potential data suggest that, for the areas tested the exclusion zone emitted PM_{10} at lower rates for equivalent wind friction speeds over the range tested. For the lowest wind friction speed tested (0.24 m/s [14 mph at 10 m]), the driving area emissions were 56% higher than in the exclosure area and at the highest wind friction speed tested (0.69 m/s [41 mph at 10 m]) the emissions in the driving area was 70% higher . Taking into account the uncertainty in the measurements, as represented by the standard deviation of the mean PM_{10} emission rate, at each of the test wind friction speeds, there is considerable overlap as indicated by the error bars in Fig. 31b that makes it difficult to assert if the difference in the mean values is meaningful. The same holds for the comparison of emissions among sites as shown in Fig. 32b and as compared in Table 5, which shows there are no statistically significant differences among emissions at the straw bale site, vegetated dune site, and the exclosure area. PI-SWERL measurements outside of the exclosure site were statistically different than those obtained at either the vegetated or straw bale site. To date the data suggests that the emissions of PM_{10} from the different parts of the Oceano dunes vary within a factor of two, and not by orders of magnitude. To more fully evaluate the difference in emission potential between the exclosure area and the driving area will require additional measurements.

10 Recommendations

Based on the pilot study results and reviewing some of the uncertainties that remain we have some recommendations for additional actions that could be pursued to provide better understanding of the Oceano Dunes dust emission system, which would allow better plans to be developed to control those emissions.

As the areal extent of the dust emission potential measurements was limited it remains un-resolved as to what the actual variability of emission potential of the larger scale dune complex may be. Currently the available data suggest that variability in PM_{10} emissions is limited at least across the pilot test areas. To better determine if the variability is restricted or if the available data reflect a bias due to the small sample size, we recommend additional PI-SWERL measurements be made along transects from the high water line inland towards the eastern edge of the park. This will allow for the determination of the existence of high emitting areas, or whether variability in emissions lies within a restricted range. Knowing which the case is will potentially impact the control strategies adopted. For example, if variability in PM_{10} emission is low then control measures applied will work equally well in reducing emissions regardless of position provided that the frequency and magnitude of the wind speed and sand flux are also similar.

Related to this is the continued uncertainty as to the relative sand transport and emission activity among different area on the dunes. Although we can now be confident that the vegetated areas (at levels approaching or exceeding that measured at the vegetation pilot study area) have low sand flux rates and low emission potential due to the roughness effect, there are only limited data available to judge the relative activity levels of sand movement in the driving area versus the exclosure area. To better evaluate how these two areas respond to the forcing of the wind to drive sand transport and dust emissions we recommend that active monitoring of wind speed and direction and sand movement be considered for each area (using Sensits and anemometer/wind vane instruments). Sites should be as similar as possible in terms of physical setting (position, exposure, etc.) to allow for comparison of activity under similar wind and environmental conditions.

The availability now of measured PM_{10} emission rates as a function of wind friction speed from the PI-SWERL measurements offers the opportunity to use dispersion modeling to evaluate how control measures could affect the downwind concentrations of PM_{10} at the observation sites. We recommend that to better inform the development of an overall control strategy a dispersion modeling exercise be undertaken to estimate how much area would need to be controlled at the dunes, given its known emission potential and wind climatology, to reach PM_{10} levels downwind of the dunes to meet the required air quality standards.

We also recommend that the PM_{10} levels measured downwind of the Oceano Dunes, which are currently assumed to be representative of perhaps a special case condition, be compared with downwind PM_{10} concentrations measured at coastal dunes in close proximity to Oceano Dunes to evaluate whether they are similar or different to dunes of similar scale under similar wind regimes. We recommend that downwind PM_{10} monitoring and meteorological measurements be considered for the Guadalupe Dunes, south of the Oceano Dunes.

11 References

Bagnold, R. A., 1941. The Physics of Blown Sand and Desert Dunes. London, Chapman and Hall.

Craig, J., Cahill, T., Ono, D., 2010. South Country Phase 2 Particulate Study. San Luis Obispo County Air Pollution Control District.

Crawley, D.M., Nickling, W.G., 2003. Drag partition for regularly-arrayed rough surfaces. Boundary-Layer Meteorology, 107(2), 445-468.

Etyemezian, V., Nikolich, G., Ahonen, S., Pitchford, M., Sweeney, M., Gillies, J., Kuhns, H., 2007. The Portable In-Situ Wind Erosion Laboratory (PI-SWERL): a new method to measure PM10 windblown dust properties and potential for emissions. Atmospheric Environment, 41, 3789-3796.

Fryrear, D. W., 1986. A field dust sampler. Journal of Soil and Water Conservation, 41, 117-120.

Gillies, J., Nickling, W.G., King, J., 2007. Shear stress partitioning in large patches of roughness in the atmospheric inertial sublayer. Boundary Layer Meteorology, 122, 367-396.

Gillies, J.A., Nickling, W.G., King, J., 2006. Aeolian sediment transport through large patches of roughness in the atmospheric inertial sublayer. Journal of Geophysical Research, 111, F02006.

Greeley, R., Iversen, J.D., 1985. Wind as a Geological Process. Cambridge University Press, Cambridge.

Hesp, P.A., 1981. The formation of shadow dunes. Journal of Sedimentary Petrology, 51, 101-112.

King, J., Nickling, W.G., Gillies, J.A., 2005. Representation of vegetation and other nonerodible elements in aeolian shear stress partitioning models for predicting transport threshold. Journal of Geophysical Research, 110(F04015).

King, J., Nickling, W.G., Gillies, J.A., 2006. Aeolian shear stress ratio measurements within mesquite-dominated landscapes of the Chihuhuan Desert, New Mexico, USA. Geomorphology, 82, 229-244.

Lancaster, N. and A. Baas, 1998. Influence of vegetation cover on sand transport by wind: field studies at Owens Lake California. Earth Surface Processes and Landforms, 25, 68-82.

Middleton, G.V., Southard, J.B., 1984. Mechanics of Sediment Movement. S.E.P.M., Tulsa, Oklahoma.

Musick, H.B., Gillette, D.A., 1990. Field evaluation of relationships between a vegetation structural parameter and sheltering against wind erosion. Land Degradation and Rehabilitation, 2, 87-94.

Okin, G.S., 2008. A new model of wind erosion in the presence of vegetation. Journal of Geophysical Research, Earth Surface, 113, F02S10.

Raupach, M.R., Gillette, D.A., Leys, J.F., 1993. The effect of roughness elements on wind erosion threshold. Journal of Geophysical Research, 98, 3023-3029.

Wolfe, S.A., Nickling, W.G., 1993. The protective role of sparse vegetation in wind erosion. Progress in Physical Geography, 17, 50-68.

Wolfe, S.A., Nickling , W.G., 1996. Shear stress partitioning in sparsely vegetated desert canopies. Earth Surface Processes and Landforms, 21(7), 607-620.